

RECONNAISSANCE LITHOGEOCHEMICAL INVESTIGATION OF THE BULL ARM FORMATION AND SIGNIFICANCE OF DIAMICTITE IN THE OVERLYING BIG HEAD FORMATION IN THE LONG HARBOUR-PLACENTIA AREA, WESTERN AVALON PENINSULA, NEWFOUNDLAND

A.J. Mills and H.A.I. Sandeman¹

Regional Geology Section

¹Mineral Deposits Section

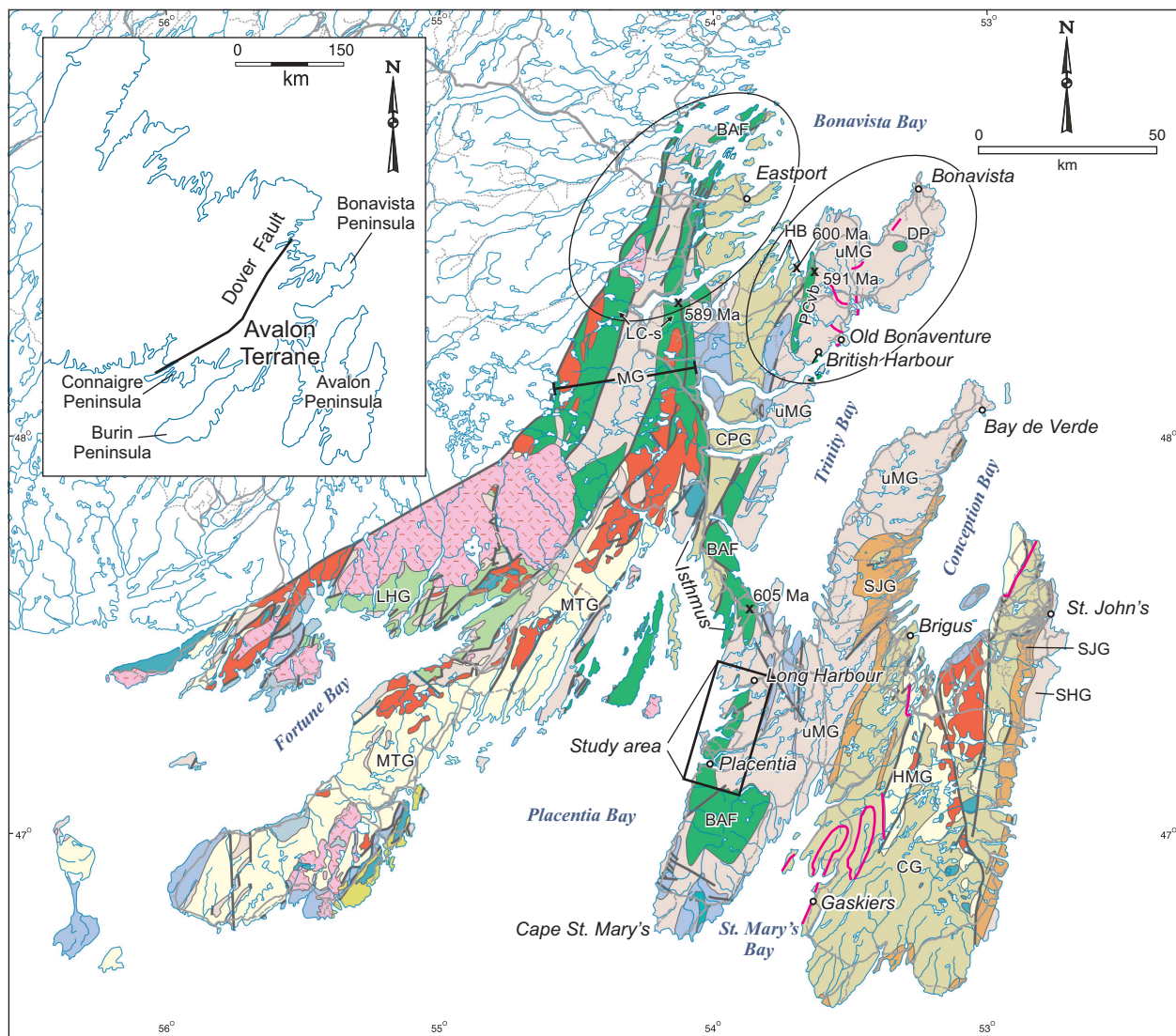
ABSTRACT

A reconnaissance lithogeochemical investigation of volcanic rocks of the Bull Arm Formation in the Long Harbour-Placentia area, western Avalon Peninsula, has identified three chemically distinct volcanic assemblages. Assemblage 1 includes green to brick-red, locally scoriaceous, weakly calc-alkaline basalt breccia, and mafic and intermediate tuffs chemically characterized by relatively steep multi-element slopes (mean La/Yb_{CN} for mafic rocks = 4.5), and significant Nb troughs (La/Nb_{CN} ~5; Th/Nb_{CN} ~9). Assemblage 2 includes mainly green, locally reddish (hematitized), amygdaloidal, plagioclase- and clinopyroxene-phyric, tholeiitic basalt flows that exhibit flatter multi-element patterns (mean La/Yb_{CN} = 3.3) and less pronounced Nb (and other HFSE) troughs (mean La/Nb_{CN} = 2.7; Th/Nb_{CN} = 4.7) than those of Assemblage 1. Assemblage 3 includes dark-grey to green-grey amygdaloidal basalt, agglomerate and volcanogenic conglomerate commonly interbedded with red mudstone, and narrow (<2 m wide), northwest-trending diabase dykes that cut massive basalt of Assemblage 2. Assemblage 3 basalts are alkaline, have the highest Mg#’s, TiO₂, V, Cr and Ni contents, exhibit multi-element patterns that lack Nb and Ti troughs, and have the steepest slopes (mean La/Yb_{CN} = 10.9) of the basaltic rocks sampled. Rocks of Assemblage 1, 2 and 3 in the Long Harbour-Placentia area are chemically similar to, and show the same relative timing of emplacement as, the basaltic rocks of the Bonavista Peninsula. Although no age constraints are currently available for the volcanic rocks in the study area, all three assemblages occur stratigraphically below a distinctive diamictite unit within the overlying Big Head Formation. The Big Head diamictite contains faceted, bullet-shaped, and flat-iron clasts and other features consistent with, although not diagnostic of, a glacial origin. The diamictite may be correlative to ca. 580 Ma diamictites of the Gaskiers Formation (Conception Group on the eastern Avalon Peninsula) and Trinity facies (Rocky Harbour Formation, Musgravetown Group on the Bonavista Peninsula), providing a possible minimum age for all three volcanic assemblages. Late Ediacaran, deep-seated alkaline magmatism (Assemblage 3 in Long Harbour-Placentia area; Dam Pond basalts in Bonavista area) along with concomitant extension and crustal thinning may have helped induce the widespread deglaciation (Gaskiers event) evident across much of the Avalon Terrane in Newfoundland.

INTRODUCTION

Neoproterozoic volcanic rocks of the Avalon Terrane in Newfoundland were traditionally assigned to the Harbour Main Group (Howell, 1920; Rose, 1952) and the Bull Arm Formation, basal Musgravetown Group (Hayes, 1948; Jenness, 1963), in the eastern and western parts of the terrane, respectively (Figure 1). A third volcanic unit, the former Love Cove Group of Jenness (1963), Dec *et al.* (1992) and O’Brien *et al.* (1996), was renamed the Broad Island Group by Mills *et al.* (2020), which refers to the spatially restricted (~2 x 6 km) remnant of a *ca.* 620 Ma Avalonian arc in northwestern Bonavista Bay that is ‘basement’ to the marine basinal Connecting Point Group. The Harbour Main Group and Bull Arm Formation form broadly north-north-

east-trending belts separated by younger siliciclastic rocks that impede direct correlation. The western volcanic unit (Bull Arm Formation) was long thought to be younger than the eastern unit because it overlies the flysch-dominated Connecting Point Group, whereas the eastern unit (Harbour Main Group) lies below the flyschoid Conception Group (Figure 2A); the flyschoid units were thought to be correlative based on similarities of thickness and lithology (*e.g.*, Buddington, 1919; Christie, 1950; McCartney, 1967; Knight and O’Brien, 1988; King, 1988; *cf.* Brückner, 1977). The Harbour Main Group is now known to be a composite unit comprising volcanic rocks of different ages, ranging from *ca.* 729 to *ca.* 580 Ma (Israel, 1998; O’Brien *et al.*, 2001; Skipton *et al.*, 2013). Recent work in the Bonavista and Eastport areas (Figure 1) has shown that the Bull Arm



AVAIL ON ZONE

DEVONIAN AND CARBONIFEROUS INTRUSIVE ROCKS

 Mainly granites: posttectonic relative to latest deformation

NEOPROTEROZOIC TO EARLY ORDOVICIAN STRATIFIED ROCKS

Shallow-marine, mainly fine-grained, siliciclastic rocks, including minor limestone and volcanic rocks

NEOPROTEROZOIC

 Fluvial and shallow-marine siliciclastic rocks (Signal Hill Group, parts of Musgravetown Group)

 Marine deltaic siliciclastic rocks (St. John's Group)

Marine turbidites (Conception and Connecting Point groups)

Gaskiers Formation, Trinity facies (glacial Conception and Musgravetown groups)

LEGEND

- [Green box] Bimodal, mainly subaerial volcanic rocks (Long Harbour Group)
 - [Dark Green box] Mainly subaerial volcanic rocks (unseparated Love Cove schist, Bull Arm and Rocky Harbour formations, Musgravetown Group)
 - [Yellow box] Submarine to subaerial volcanic rocks (Harbour Main, Connraighe Bay, Marystown and Broad Island groups)
 - [Orange box] Pillow basalt, mafic volcanioclastic rocks, minor siliciclastic rocks, limestone and chert (Burin Group)

NEOPROTEROZOIC TO CAMBRIAN INTRUSIVE ROCKS

- Mafic intrusions
Granitoid intrusions, including unseparated mafic phases

SYMBOLS

- Geological contact, Fault
Town, U-Pb (zircon) age

Figure 1. Simplified geology of the Avalon Terrane in Newfoundland showing the study area, and age constraints for Bull Arm Formation rocks from the Isthmus, Eastport and Bonavista areas. Modified from Colman-Sadd et al. (1990) and incorporating changes suggested by Mills et al. (2020). BAF = Bull Arm Formation; (u)MG = (upper) Musgravetown Group; LC-s = Love Cove schist; LHG = Long Harbour Group; MTG = Marystown Group; CPG = Connecting Point Group; CG = Conception Group; SJG = St. John's Group; SHG = Signal Hill Group; HMG = Harbour Main Group; HB = Headland basalt; DP = Dam Pond basalt; PCvb = Plate Cove volcanic belt (geographic name for Bull Arm Formation volcanic rocks on Bonavista Peninsula).

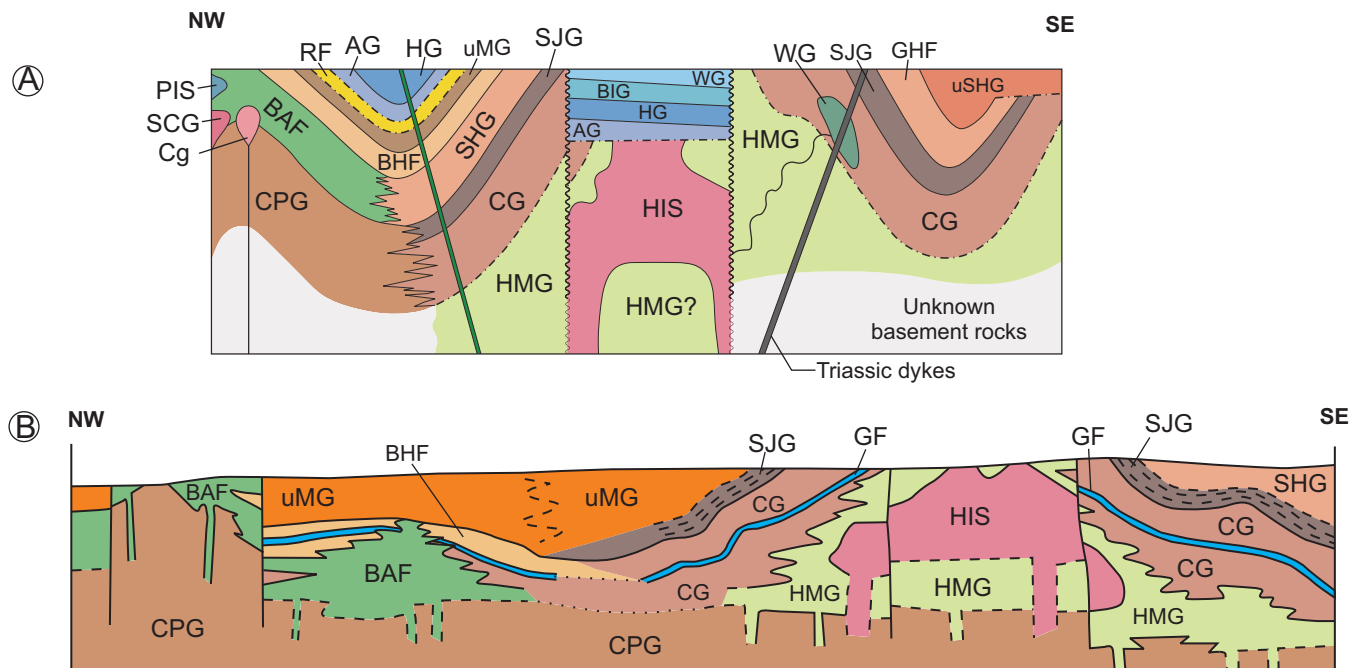


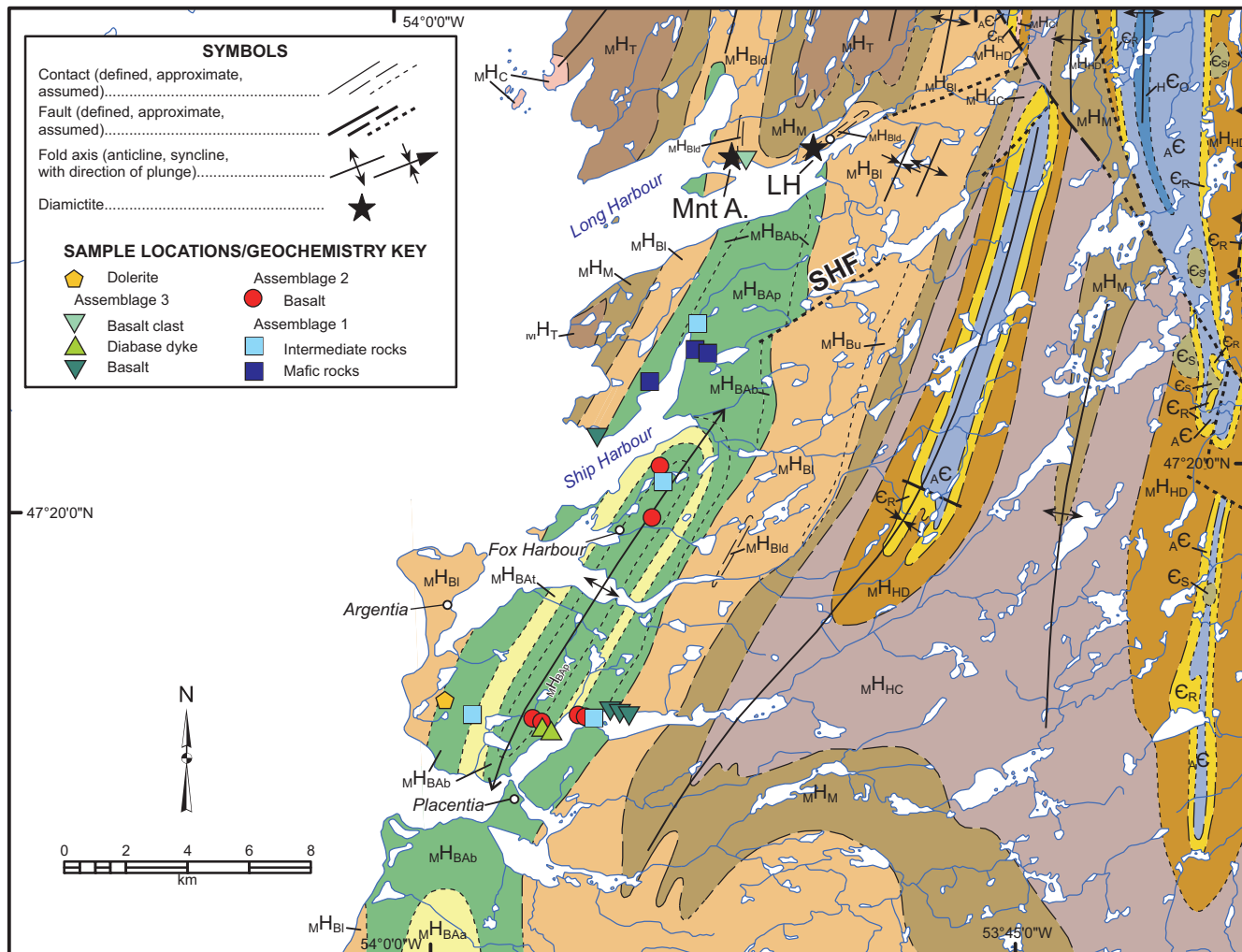
Figure 2. Previously proposed schematic cross-sections through the Avalon Terrane in Newfoundland. A) After King (1988); B) After Brückner (1977). Glacial diamictite occurs within CG on 'A' and as thin blue line within CG and BHF on 'B'. AG = Adeyton Group; BIG = Bell Island Group; HG = Harcourt Group; RF = Random Formation; BAF = Bull Arm Formation; BHF = Big Head Formation; uMG = upper Musgravetown Group; CPG = Connecting Point Group; CG = Conception Group; Cg = Clarenville granite; GF = Gaskiers Formation; SJG = St. John's Group; GHF = Gibbett Hill Formation (lower Signal Hill Group); uSHG = upper Signal Hill Group; HMG = Harbour Main Group; HIS = Holyrood Intrusive Suite; WG = Wabana Group; PIS = Powder Horn Intrusive Suite; SCG = Swift Current granite.

Formation also comprises rocks of different ages and petrochemical characteristics (Mills and Sandeman, 2015; Mills *et al.*, 2017, 2020). As the upper components of both the Harbour Main Group and Bull Arm Formation are overlain by *ca.* 580 Ma glaciogenic diamictite (Pu *et al.*, 2016), previous stratigraphic nomenclature and regional correlations across the Avalon Terrane in Newfoundland (*e.g.*, McCartney, 1967; King, 1988) must be re-evaluated and revised (see Figure 2).

This contribution focuses on the lithogeochemistry of the Bull Arm Formation in the Long Harbour–Placentia area (McCartney, 1967; King, 1988) and aims to: 1) establish the chemical character of the volcanic rocks in the study area; 2) discern whether the formation comprises rocks of one or more lithogeochemical signature(s); and 3) to establish the relative timing of emplacement of its constituent assemblage(s). In addition, field descriptions are included for diamictites from two localities in the Long Harbour area (*see also* Brückner, 1977) and the regional significance of these rocks is highlighted. This investigation is based upon field and petrographic observations and lithogeochemistry for 21 samples from 13 sites (Figure 3).

REGIONAL GEOLOGY

The Long Harbour–Placentia area is situated south of the Isthmus of Avalon on the west side of the Avalon Peninsula, or the northern part of the Cape St. Mary's sub-peninsula (black box, Figure 1). The area is underlain by mainly volcanic and clastic sedimentary rocks of the Bull Arm and Big Head formations, respectively (McCartney, 1967; King, 1988). The study area was previously mapped at $\sim 1:50\,000$ scale (Argentia map sheet; McCartney, 1956), compiled with adjacent maps at 1 inch to four miles (McCartney, 1967), and recompiled at 1:250 000 (King, 1988). The mainly volcanic Bull Arm Formation is the stratigraphically lowest unit in the area and includes andesite to basalt flows and breccias, intercalated tuff, red and green arkose, siltstone, slate, conglomerate and minor rhyolitic lava flows and breccias (*see* McCartney, 1956, 1967). It occupies the core of a northeast-trending anticline south of Long Harbour, interpreted by King (1988) to be doubly-plunging (Figure 3). Only small slivers of the Bull Arm Formation outcrop north of the Long Harbour inlet. The volcanic rocks are overlain by predominantly fine-grained clastic sedimentary rocks of the Big Head Formation, Musgravetown Group (McCartney, 1967; King,



LEGEND

SPREAD EAGLE GABBRO (and equivalents)	
E_S	Diabase and gabbro (may feed Cambrian volcanic rocks)
HARCOURT GROUP	
H_C	Mainly black shale
ADEYTON GROUP	
A_C	Mainly green and red shale, minor limestone
RANDOM FORMATION	
R_R	White orthoquartzite interbedded with green, grey and red arkose and siltstone; local basal conglomerate
MUSGRAVETOWN GROUP	
CROWN HILL FORMATION	
M_Hc	Red pebble conglomerate and sandstone; locally, red siltstone at base; minor green conglomerate
TRINNY COVE FORMATION	
M_Ht	Olive-green and red sandstone, siltstone and conglomerate; minor grey shale containing wispy sandstone laminae
HEART'S DESIRE FORMATION	
M_Hd	Olive-green sandstone
HEART'S CONTENT FORMATION	
M_Hc	Grey to black shale containing wispy sandstone laminae
MATURIN PONDS FORMATION	
M_Hm	Red sandstone and mudstone exhibiting distinctive wavy bedding; minor conglomerate
BIG HEAD FORMATION	
M_Hbu	Grey to red arkose and granule conglomerate
M_Hbl	Wavy bedded, grey to green tuffaceous siltstone and arkose; locally includes Whiteway Member consisting of red sandstone and siltstone
M_Hbld	Green-grey to maroon volcanogenic mixtite or diamictite
BULL ARM FORMATION	
M_Hbaa	Felsic flows and tuffs, and clastic sedimentary rocks
M_Hbab	Mafic flows; includes minor felsic flows and clastic sedimentary rocks
M_Hbat	Predominantly crystal and lithic tuffs, commonly reworked
M_Hbap	Mafic to felsic variegated flows, and pyroclastic and clastic sedimentary rocks

Figure 3. Geology of the Long Harbour–Placentia area showing the sample locations. Modified from King (1988). Key: Mnt A. = Mount Arlington Heights; LH = community of Long Harbour; SHF = Ship Harbour fault.

1988). A distinctive diamictite unit occurs roughly in the middle of the Big Head Formation and is exposed on the east and west limbs of a syncline, at the communities of Long Harbour and Mount Arlington Heights, respectively (Brückner, 1977; MHBID unit of King, 1988). The Big Head Formation is overlain by redbeds of the Maturin Ponds Formation (McCartney, 1967; King, 1988).

AGE AND CHEMICAL CONSTRAINTS ON THE BULL ARM FORMATION

No age constraints are, as of yet, available for rocks of the Bull Arm Formation on the western Avalon Peninsula. In the Isthmus of Avalon, and Bonavista and Eastport peninsulas, U-Pb (zircon) geochronological and lithogeochemical studies have shown a time-progressive change in the chemistry of magmatic Musgravetown Group rocks, formerly all included in the Bull Arm Formation. On the Isthmus of Avalon, 20 km south of the type locality of Bull Arm (Figure 1), the banded rhyolite having transitional (between calc-alkaline and alkaline) chemistry has been dated at *ca.* 605 Ma, is considered basal Musgravetown Group, and is overlain by tholeiitic and alkaline basalts (Mills *et al.*, 2017, 2020).

On the Bonavista Peninsula, *ca.* 600 Ma basal Musgravetown Group cobble- to boulder-conglomerate (Cannings Cove Formation; Jenness, 1963) and interbedded calc-alkaline basalt (Headland basalt of Mills and Sandeman, 2015) unconformably overlie *ca.* 605 Ma shallow-marine rocks of the upper Connecting Point Group (Mills *et al.*, 2016). Bull Arm Formation rocks outcrop farther east (Figure 1), in the internally deformed and steeply east-dipping Plate Cove volcanic belt, which broadly separates the Connecting Point Group (620–605 Ma; Mills *et al.*, 2020) to the west from Musgravetown Group rocks to the east (*e.g.*, Jenness, 1963; Mills, 2014). The chemically transitional (tholeiitic to weakly calc-alkaline) basalts of the belt are interpreted as continental tholeiites that erupted in a tensional or transtensional setting (Mills and Sandeman, 2015). The transitional chemistry of Bull Arm Formation magmatism marks a change from early arc-like magmatism to later extension-related magmatism (Mills *et al.*, 2020). Although the basalts from the Plate Cove volcanic belt have not been dated, felsic tuffaceous rocks from the west and east side of the belt yielded ages of 592 ± 2.2 Ma and 591.3 ± 1.6 Ma, respectively (Mills *et al.*, 2017). The basalts are interpreted to be similar in age to the dated tuffs. Alkaline basalts in the northeastern (Dam Pond) and southwestern (British Harbour) parts of the Bonavista area (Figure 1) occur below and above, respectively, the Trinity facies (Normore, 2011), a glacial diamictite unit dated at 580 Ma near Old Bonaventure and correlative to the 580-Ma Gaskiers Formation (Williams and King, 1979; Pu *et al.*, 2016).

In the Eastport area, earliest magmatism is calc-alkaline and includes felsic to intermediate tuff of the *ca.* 620 Ma Broad Island Group and younger mafic flows, dykes and schist of the Cannings Cove Formation (Mills *et al.*, 2020). The Love Cove schist (Widmer, 1949; *see also* Dec *et al.*, 1992) is 589 ± 2 Ma at its type locality (*see* Figure 1 for location), and these chemically transitional pyroclastic rocks are interpreted to be strongly tectonized correlatives of the Bull Arm Formation (Mills *et al.*, 2020). Alkaline rocks in the Eastport area, including the 568.7 ± 1.4 Ma Wolf Island rhyolite, are part of the younger Rocky Harbour Formation (O'Brien and King, 2004; Mills *et al.*, 2020).

In summary, Musgravetown Group magmatism on northwestern Avalon Terrane in Newfoundland includes *ca.* 600 Ma and older calc-alkaline magmatism, *ca.* 589 Ma and older tholeiitic and transitional magmatism (Bull Arm Formation), and *ca.* 580–569 Ma alkaline magmatism (Rocky Harbour Formation).

PREVIOUS FIELD DESCRIPTIONS OF DIAMICTITE WITHIN THE BIG HEAD FORMATION, LONG HARBOUR–MOUNT ARLINGTON HEIGHTS AREA

Tillite was reported in the Big Head Formation at Long Harbour and Mount Arlington Heights by Brückner (1977). Whereas ‘tillite’ is today defined as “unsorted sediment deposited directly from glacier ice” (Hambrey and Glasser, 2012), its connotation in 1977 more loosely included “rocks of glacial origin” (Brückner, 1977). Big Head, on the north shore of the inlet of Long Harbour, is the type area for the Big Head Formation and is divided by McCartney (1967) into three subdivisions: lower “red conglomerate and arkose beds” (interpreted by Brückner (1977) as pyroclastic deposits ranging from breccias to graded tuffs); medial grey-green siliceous siltstone, chert and minor arkose; and upper, green to locally pinkish arkose. The distinct diamictite beds occur within McCartney’s (1967) middle division. Brückner (1977) estimates the diamictite (his “tillite bed”) thickness to be 15–20 m at Long Harbour and ~10 m at Mount Arlington Heights. The lower contact is not exposed at either location. The upper contact is exposed only at the Mount Arlington site, where it grades into bedded chert without clasts (Brückner, 1977). Clasts in the diamictite are unsorted, range from angular to rounded, 5–12 cm in diameter, and mainly consist of mafic or felsic volcanic lithologies with lesser fragments of vein quartz, arkose and siltstone. Brückner (1977) suggested that the volcanic clasts in the diamictite were all locally derived from rocks of the underlying Bull Arm Formation. Although he did not discern glacial striae on the clast surfaces, he asserts that the poor sorting of both clasts and matrix material, the range of

clast lithology, shape and size, and the general appearance of the Long Harbour diamictite, which “so closely resemble those of the Gaskiers tillite”, are sufficient criteria upon which to interpret the former as “genuine tillite”.

NEW FIELD OBSERVATIONS OF DIAMICTITE WITHIN THE BIG HEAD FORMATION, LONG HARBOUR–MOUNT ARLINGTON HEIGHTS AREA

Whereas most of Brückner’s (1977) observations come from the hilltop at Mount Arlington (immediately north and east of the Mount Arlington diamictite location on Figure 3), new observations documented here come from the rock-cut along the north side of the road at the base of the same hill. The lowermost strata there comprises sandy mudstone with <1% dispersed clasts (classification scheme of Hambrey and Glasser, 2012). Laminated maroon mudstone is interbedded at mm- to cm-scale with medium- to coarse-grained grey sandstone layers and lenses, and the rock locally contains outsized (3–10 mm), red cherty clasts (Plate 1A). Sandstone lenses commonly pinch-out laterally over distances of 5–20

cm or are truncated by overlying layers (Plate 1A). The nature, thickness and lateral continuity of these beds/laminae vary along strike; planar, wavy, lenticular and slumped beds or laminae all occur within 10s of metres along strike. A disconformity (Plate 1B) marked by pebble to boulder, porphyritic and/or amygdaloidal basalt clasts (pebble lag or lapilli/bombs?) occurs close to the transition between underlying maroon mudstone–grey sandstone facies and overlying green-grey laminated mudstone ± sandstone facies (Plate 1C). The overlying green-grey mudstone ± sandstone facies (Plate 2) is highly siliceous and is characterized by sub-mm-scale rhythmic laminations in the mudstone (Plate 3A). Compared to the underlying maroon facies, sandstone beds in the upper facies are thicker (dm-scale), have more pebbles and contain more outsized clasts. Outsized clasts comprise 1–3% of the green-grey laminated mudstone and up to 15% of the sandstone. Compositionally, the clasts include sandstone, chert, laminated siltstone, basalt and rare rhyolite or felsite (Plate 2A). Pebby sandstone occurs as 20–50-cm thick beds, as discontinuous lenses up to m-scale in width and as sandstone dykes up to 10 cm long (Plate 3B). Laminae typically deflect around the clasts (Plate 4A), which themselves range from angular to rounded. Flat-iron

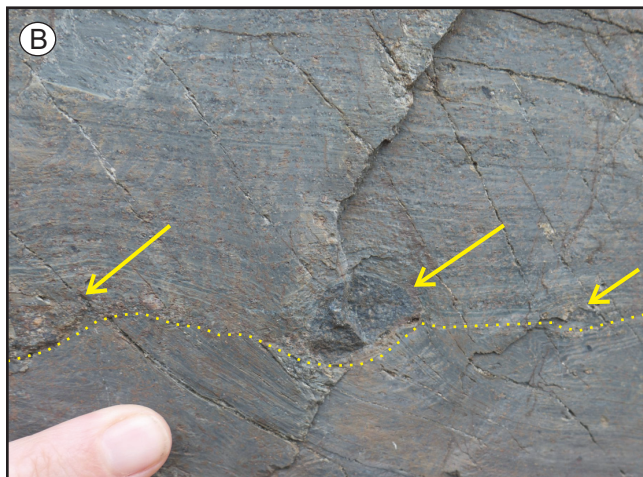
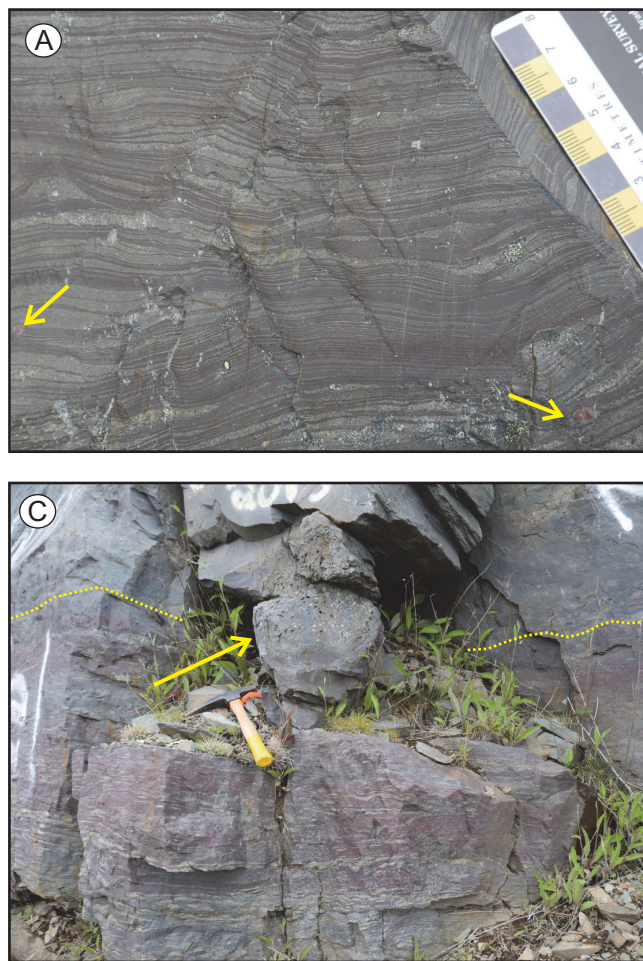


Plate 1. Field photographs of rocks in the Mount Arlington Heights area. A) Wavy-bedded, finely laminated maroon mudstone interbedded with layers and lenses of fine- to coarse-grained grey sandstone and containing dispersed small (3–6 mm) pebbles of red chert (yellow arrows); B) Discontinuity (dotted yellow line) marked by pebble lag comprising mainly porphyritic basalt clasts (yellow arrows); C) Boulder of amygdaloidal basalt (lithogeochemistry sample 19AM001; Assemblage 3) at the transition between maroon mudstone–grey sandstone facies and overlying green-grey laminated mudstone–sandstone facies.

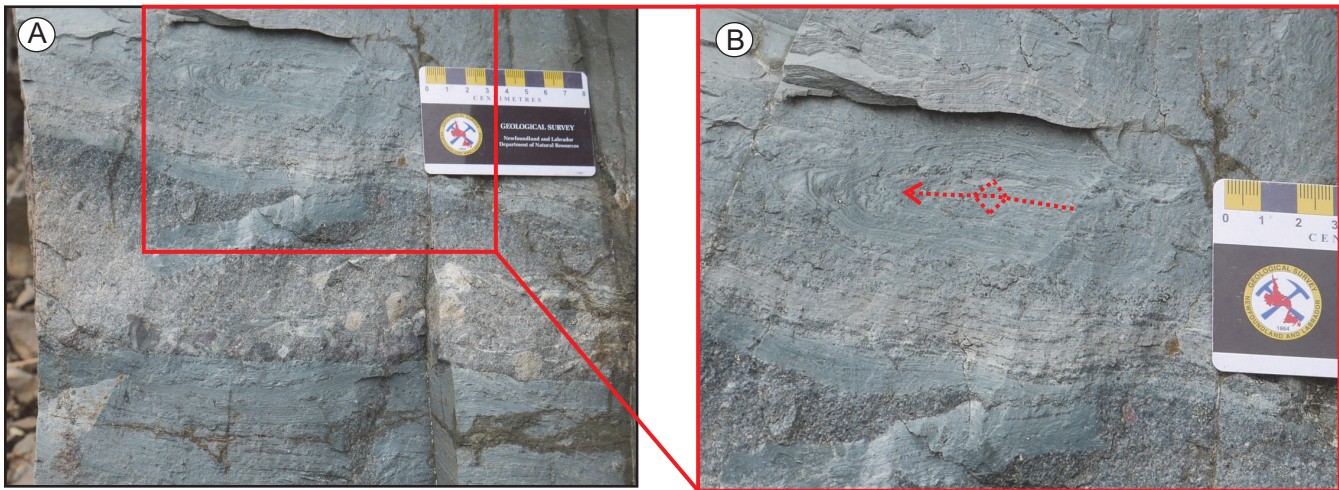


Plate 2. A) Green-grey laminated mudstone–sandstone facies at Mount Arlington Heights having subangular to subrounded clasts of mudstone, siltstone, sandstone, basalt and rhyolite/felsic tuff, and showing B) sheath fold in laminated green-grey mudstone (red dashed arrow shows antiformal geometry of the fold).

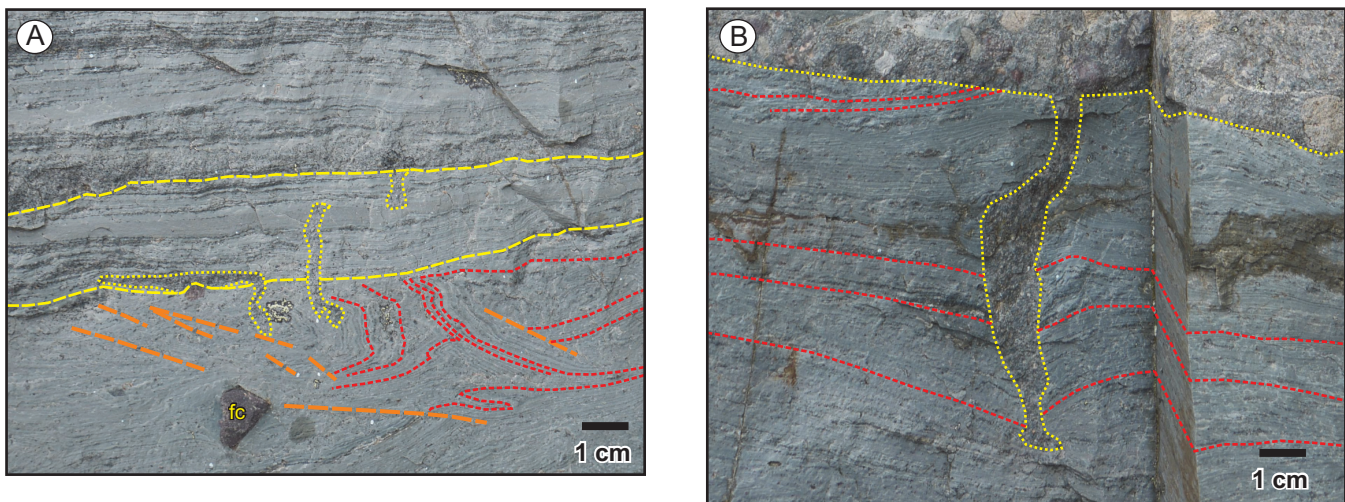


Plate 3. Close-up photographs of green-grey laminated mudstone–sandstone facies from Mount Arlington Heights. A) Finely laminated, green-grey siliceous mudstone–sandstone showing truncated layers (truncating layers shown as dashed yellow lines), folded and slumped laminae (dashed red lines), sandstone dykes and sills (dotted yellow lines), weakly developed shear bands (orange dashed lines), and an outsized (>1 cm) faceted clast (fc); B) Finely laminated green-grey mudstone scoured and truncated by overlying pebbly sandstone; note ~9 cm long sandstone dyke.

(Plate 4A), faceted (Plate 3A) and bullet-shaped (Plate 4A) clasts (Boulton, 1978) are common. Bedding-confined slumps, convolutions, sheath folds and possible glaciodislocations (Chumakov, 2015) are also common in the laminated mudstone (Plates 2B and 3A).

A few small (<5 m in length) outcrops were investigated at Long Harbour and these differ lithologically from those at Mount Arlington Heights. Specifically, the Long Harbour outcrops consist of green-grey, massive, clast-poor

to clast-rich, intermediate diamictite (poorly sorted, matrix-supported conglomerate having a sand-to-mud ratio between 33–66%; Hambrey and Glasser, 2012). Diffuse, pale-green bands were noted (Plate 4B). The pale bands could result from a compositional difference and, if so, may indicate that the rock is crudely stratified. However, these bands could also result from patchy alteration, as they tend to be sparse, and are commonly irregular and discontinuous. Clasts range from granules to cobbles and are most commonly basalt (Plate 4B), although pink felsite or chert,

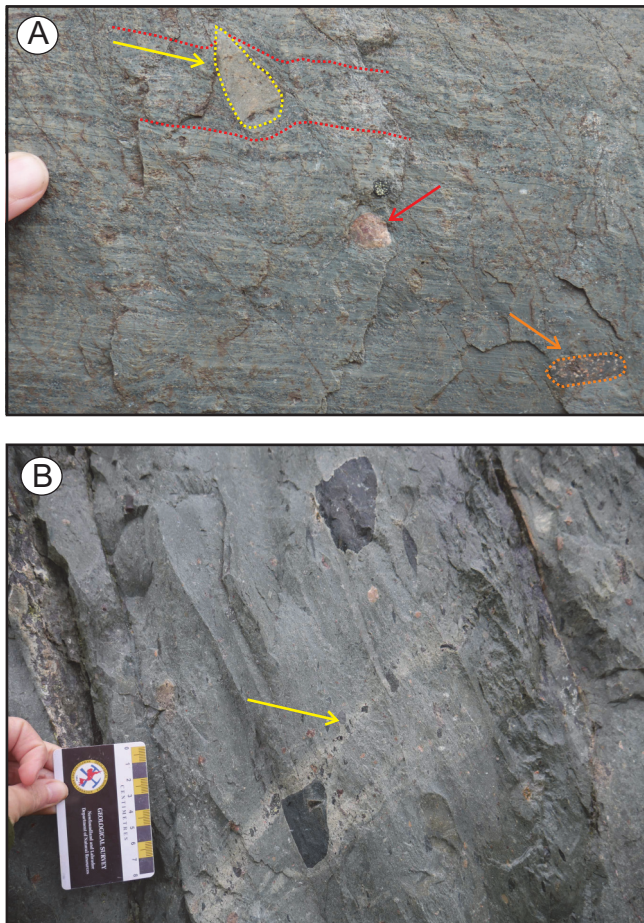


Plate 4. Further examples of possible peri-glacial deposits from the study area. A) Finely laminated green-grey siliceous mudstone-sandstone facies from Mount Arlington showing outsized clasts with rounded (red arrow), flat-iron (yellow arrow, dotted line), and bullet-shaped (orange arrow, dotted line) morphologies; B) Clast-poor intermediate diamictite with cobble-sized clasts of basalt; yellow arrow indicates the diffuse pale-green banding common in outcrops in the vicinity of the community of Long Harbour.

green-grey sandstone, siltstone, and rare quartzite clasts were also noted. The thickness of the diamictite at Long Harbour was not ascertained, but Brückner's (1977) estimate of 15–20 m is consistent with field observations. A variably developed, subvertical cleavage is locally accentuated by flattened black lithic fragments.

FIELD AND PETROGRAPHIC OBSERVATIONS OF THE BULL ARM FORMATION, LONG HARBOUR-PLACENTIA AREA

Twenty-one samples were collected from the Long Harbour-Placentia area (Figure 3) for lithogeochemical

analysis, including four samples collected in 2017 by the second author. Brief petrographic descriptions are presented in Table 1. All samples, with one exception, were collected from rocks mapped as Bull Arm Formation (McCartney, 1956, 1967). The single exception is an amygdaloidal basalt boulder sampled from the diamictite unit within the overlying Big Head Formation (Plate 1C) at Mount Arlington Heights. The Bull Arm Formation is generally poorly exposed over an elongate, north-northeast-trending, 5–6 km wide by 16 km long, antiformal structure cored by mainly basaltic rocks (Figure 3). The samples include massive basalt flows, pyroclastic rocks including scoriaceous basalt and a range of tuffaceous rocks, the amygdaloidal basalt boulder from the base of the diamictite at Mount Arlington Heights, two basaltic dykes cutting massive basalt, and a dolerite that lacks exposed contacts.

The subdivision of the rocks exposed in the Bull Arm Formation antiform between the communities of Long Harbour and Placentia (Figure 3) based on lithofacies alone is problematic owing to the variability and heterogeneity of the formation's constituent lithologies. Therefore, an informal subdivision of Bull Arm Formation strata into three assemblages is proposed based on petrology and lithogeochemistry.

Assemblage 1 includes green to brick-red fragmental basaltic rocks or breccias (Plate 5A), and crystal lithic, crystal ash (Plate 5B), and lapilli tuffs. Assemblage 2 includes mainly green, locally hematitized to reddish, amygdaloidal, plagioclase- and clinopyroxene-phyric basalt flows (Plate 5C). Assemblage 3 includes dark-grey to green-grey amygdaloidal basalt, green-grey to red fragmental basalt interbedded with basalt-clast-bearing red mudstone (Plate 5D) and narrow (30–200 cm wide), northwest-trending, subvertical basalt dykes that cut massive basalt of Assemblage 2 (Plate 5E). Igneous rocks of all three assemblages are interbedded with sandstone, siltstone, mudstone and pebble conglomerate with no clear lithological association distinctive to any particular volcanic assemblage. Variably hematitized fragmental basalt occurs within assemblages 1 and 3. Rocks of Assemblage 2 are massive, not fragmental, but reddening/hematitization was noted locally.

In thin section, polycrystalline chlorite appears to have completely replaced possible mafic volcanic fragments in intermediate lithic ash tuff of Assemblage 1 (Plate 6A). Fragmental basaltic rocks of Assemblage 1 contain highly vesicular to scoriaceous fragments in a glassy groundmass. These rocks contain abundant plagioclase; no primary mafic minerals were identified in thin section. Basalts of Assemblage 2 are commonly clinopyroxene-bearing, exhibit variably developed trachytic textures, and contain rare sieve-textured plagioclase phenocrysts (Plate 6B). The

Table 1. Location data and field and petrographic descriptions of samples from the Long Harbour–Placentia area

Lab#	Sample#	Rock Type	UTM East	UTM North	Zone	Datum	Field Description	Petrographic Description
10740338	19AM012A01	basalt	273858	5239741	22	NAD 27	Dolerite from Argentia; hypabyssal texture, possible dyke or sill; margins not exposed	Gabbro – Pl + Cpx; ophitic texture – Pl laths completely embedded in Cpx; well preserved/fresh; minor interstitial Chl
Assemblage 3								
10740328	19AM006B01	basalt	276705	5238564	22	NAD 27	30–50 cm thick diabase dyke crosscuts basalt flows; trends 350/70	Tiny, equant Cpx in groundmass + Pl + opaque; 2 mm Chl blebs = possible Cpx pseudomorphs
10740329	19AM006B02	basalt	276705	5238564	22	NAD 27	1.5–2 m thick dyke cuts locally epidotized basalt; trends 31/080	Similar to 19AM006B01 but more strongly altered; possible prehnite prehnite associated with Chl+Cal
10740324	19AM001A01	clast	284067	5256514	22	NAD 27	Amygdaloidal basalt boulder in diamictite; ~20 cm diameter	Altered Pl, fine matrix; trace Ti; amygdales filled mainly with Qtz, Cal
10740337	19AM011A01	basalt	279603	5247991	22	NAD 27	Amygdaloidal basalt flow at Ship Harbour; contacts not exposed; massive/structureless	Rare 1–2 mm Cpx phenocrysts; common 2+ mm amygdales filled with Chl + Cal; possible Ep after Cpx pseudomorphs (1–2 mm)
10740346	19AM018A01	mafic agglomerate	278931	5238962	22	NAD 27	Subrounded to angular volcanic fragments in fine-grained, brick-red matrix	Matric volcanic fragments in glassy groundmass; minor carbonate blebs and veinlets
10740347	19AM018A02	mafic agglomerate	278931	5238962	22	NAD 27	Grey-green basalt bomb in red mudstone; west outcrop	Altered, sub-anhedral Pl phenocrysts; black, very-fine-grained needles (rutile?); carbonate and black (glass?) infilling veinlets
10740348	19AM018A03	mafic	278931	5238962	22	NAD 27	Grey-green basalt bomb in red mudstone; east outcrop	Trachytic textured basalt; foamy/bubbly textured fragments and spherical opaques = volcanic glass (?)
Assemblage 2								
8941358	HSI7-091C	massive basalt	281410	5446712	22	NAD 27	Dark green, medium-grained, locally pebbly sandstone with <1 m thick yellowish siltstone beds, overlain by fine-medium-grained massive basalt	Weak flow alignment of subhedral Pl; Chl interstitial to Pl, possibly replacing mafic phase(?), elongate and irregular – likely not tectonically flattened (welded tuff?); common Ti
8941355	HSI7-094	basalt	281014	5245123	22	NAD 27	Massive, medium-grained, epidotized, hematitized massive basalt	Optical continuity of Cpx in cross-polar light indicates crystals are up to 4 mm; Chl in amygdales, rimmed by Ep; rare Ti
10740326	19AM006A01	basalt	276705	5238564	22	NAD 27	Massive basalt, locally epidotized; crosscut by dykes	Pl+phyric basalt; possible Cpx inclusions in Pl; flow texture
10740327	19AM006A02	basalt	278459	5239015	22	NAD 27	Massive basalt near dyke margin; possible chill zone	Fine-grained basalt; Pl+Cpx poorly preserved phenocrysts; abundant opaques; Ep+Chl in amygdales, veinlets and blebs
10740331	19AM007A01	basalt	278459	5239015	22	NAD 27	Amygdaloidal basalt flow west of Dunville	Pl+phyric basalt (sieve-textured phenocrysts); common Chl and patchy Cal in groundmass; Ep+Chl in veinlets, fractures
10740332	19AM007A02	basalt	278459	5239015	22	NAD 27	Amygdaloidal basalt flow west of Dunville	
Assemblage 1 (tuffs)								
8941345	HSI7-093	lithic tuff	282858	5251015	22	NAD 27	Ksp-bearing lithic tuff overlies pebbly sandstone	Altered subhedral Fsp, minor felsic volcanic fragments, turbid matrix
10740325	19AM005A01	lithic ash tuff	274723	5239179	22	NAD 27	10 cm thick tuff horizon interbedded with green-grey, fine-grained sandstone and siltstone	~1 mm Chl blebs, possibly replacing matrix fragments, in very fine-grained, strongly altered (turbid) matrix
10740333	19AM007B01	crystal lithic tuff	278459	5239015	22	NAD 27	Thin tuff overlying basalt flow, west of Dunville	Crystal lithic tuff; anhedral Fsp-rich; minor basalt, siltstone clasts
10740334	19AM008A01	crystal lithic tuff	281502	5246520	22	NAD 27	Grey to maroon crystal tuff; overlain by laminated siltstone	Sedimentary and volcanic fragments in sericite/fine mica-rich (possibly originally ash?) matrix
Assemblage 1 (mafic breccias)								
8941359	HSI7-092A	basalt breccia	281287	5249524	22	NAD 27	Reddish basalt capped by flow top breccia or volcanic conglomerate with amygdaloidal basalt clasts	Basaltic fragmental; some fragments have found Ti in Chl groundmass; strongly altered Fsp; patchy carbonate
10740335	19AM009A01	basalt breccia	282803	5250513	22	NAD 27	Scoraceous mafic fragmental rock; brick red fragments, interstitial quartz, calcite and epidote	Glassy basalt fragments – pl microfossils with quench textures; voids between fragments filled with Qtz, Cal, Ep
10740336	19AM009B01	basalt breccia	282803	5250513	22	NAD 27	Green-grey basalt fragments in brick-red matrix	Scoraceous fragmental basalt; foamy/highly vesicular fragments in glassy groundmass; voids filled with altered Fsp + Qtz

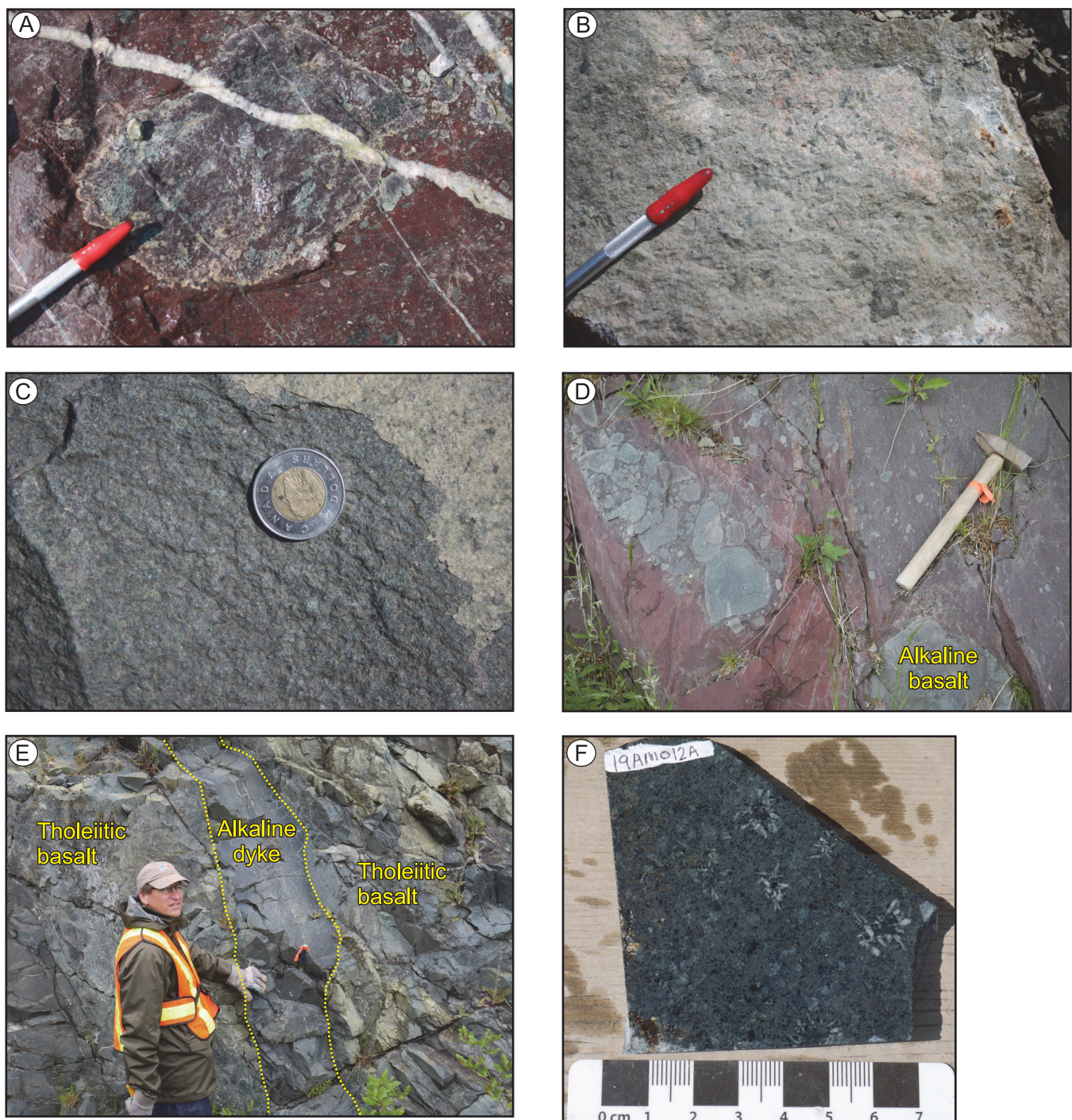


Plate 5. Field photographs of igneous rocks sampled from the study area. A) Amygdaloidal basalt clast in basaltic fragmental rocks (possible flow-top breccia; HS17-092A; Assemblage 1 mafic volcanic rock); B) Potassium feldspar-bearing lithic tuff (HS17-093; Assemblage 1 intermediate tuff); C) Weakly epidotized and hematitized massive basalt (HS17-094; Assemblage 2); D) Basalt breccia interbedded with red mudstone (19AM018A; Assemblage 3); E) 30–50 cm thick alkaline dyke (trend: 320/70) with distinct chill margins cuts patchily epidotized massive tholeiitic basalt (19AM006B01 of Assemblage 3, and 19AM006A01 of Assemblage 2, respectively), view to the north; F) Cut slab of dolerite from Argentia showing radial plagioclase glomerocrysts (19AM012A).

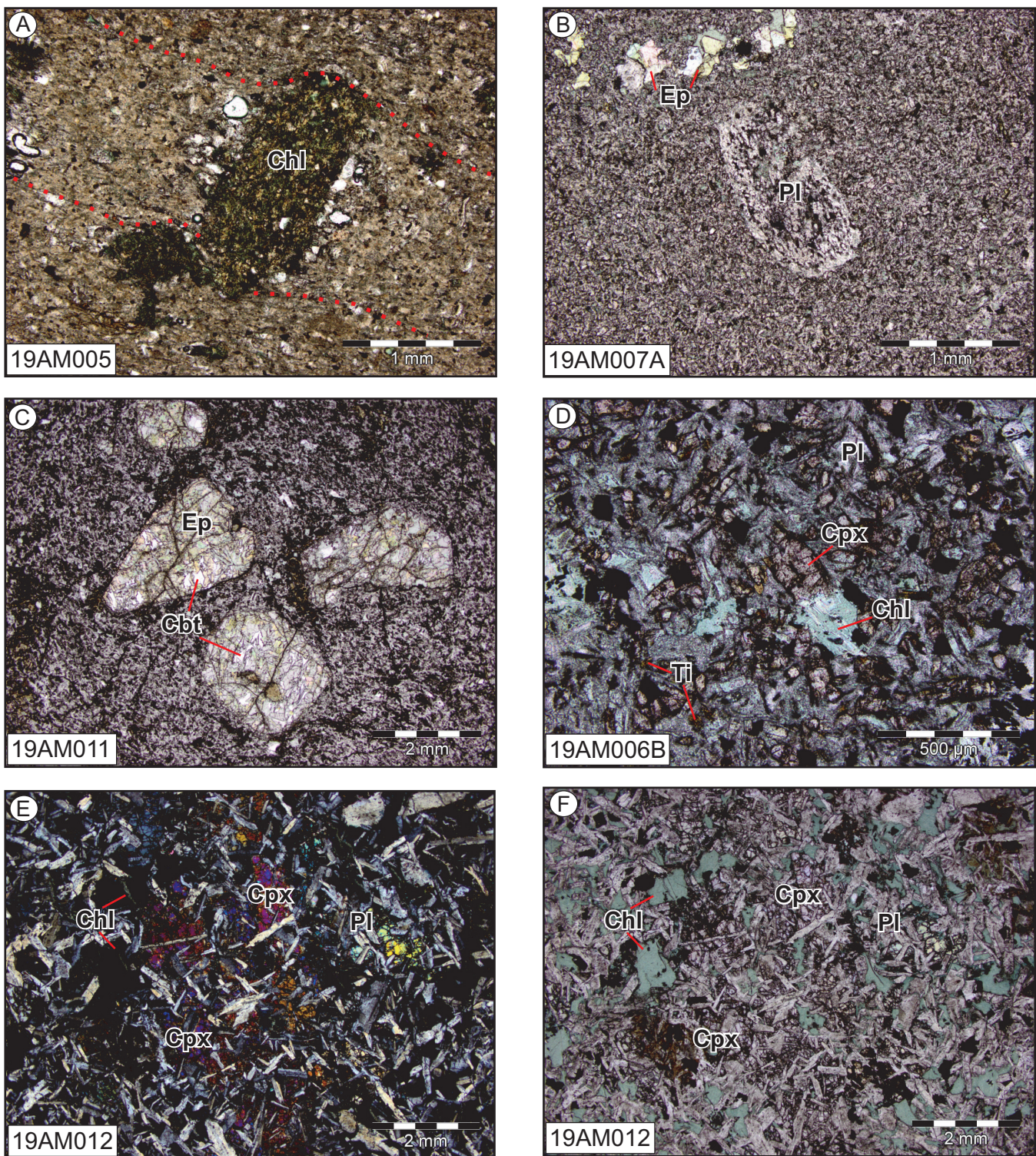


Plate 6. Photomicrographs of rocks sampled from the study area. A) Polycrystalline chlorite (*Chl*) bleb interpreted to have replaced a mafic volcanic fragment in lithic ash tuff; the red dotted lines highlight primary layering (19AM005; Assemblage 1 intermediate tuff); B) Sieve-textured, subhedral plagioclase phenocryst (*Pl*) and epidote (*Ep*) crystals (late with respect to crystallization of the rock; possibly filling amygdales) in fine-grained, weakly trachytic, plagioclase-rich groundmass (19AM007A; Assemblage 2); C) Amygdaloidal basalt from Ship Cove showing probable primary clinopyroxene crystals entirely pseudomorphed by epidote and carbonate (*Cbt*) (19AM011A01; Assemblage 3); D) Titanite (*Ti*) and clinopyroxene microphenocryst (*Cpx*) which is partially replaced by chlorite in alkaline dyke (19AM006B01; Assemblage 3); E, F) Dolerite from Argentia showing ophitic texture, best viewed under cross-polars where optical continuity of the clinopyroxene oikocryst highlights the size of the crystal; viewed in cross-polar and plane-polar light, respectively.

Assemblage 3 basalt from Ship Harbour (Figure 3) contains subhedral, 2–3 mm clinopyroxene phenocrysts, pseudomorphed by polycrystalline epidote and plagioclase, and 2–5 mm amygdalites filled with mainly chlorite and/or carbonate (Plate 6C), set in a trachytic textured fine-grained groundmass. Assemblage 3 basalt dykes contain clinopyroxene crystals partially replaced by chlorite, strongly altered (saussuritized) plagioclase, minor magnetite and titanite (Plate 6D). Large (up to 1 cm) amygdalites are most common in assemblages 2 and 3, although fragments in Assemblage 1 rocks are highly vesicular or scoriaceous. Basalts of assemblages 1 and 3 both have variably glassy groundmasses and plagioclase microlites that indicate quenching. Trachytic textures were observed locally in all three assemblages.

A dolerite sampled at Argentia has unexposed contacts; a cut slab shows glomeroclastic plagioclase crystals radiating from a central black mass (Plate 5F). In thin section, the rock exhibits well developed ophitic to subophitic texture, with elongate prismatic to acicular plagioclase chadacrysts partially to completely embedded within 2–8 mm clinopyroxene oikocrysts (Plate 6E, F). Glomeroclastic plagioclase crystals are larger than the chadacrysts (2–5 mm vs. <1 mm), and radiate out from a central mass of polycrystalline chlorite and carbonate (Plates 5F and 6E, F).

LITHOGEOCHEMISTRY

Twenty-one rock samples were collected for lithogeochemical analysis. Assemblage 1 includes three basaltic breccias and four tuffaceous rocks; Assemblage 2 includes six basalts; Assemblage 3 includes one basalt flow (from Ship Harbour; *see* Figure 3 for location), three fragmental basalts, two basalt dykes and the amygdaloidal basalt boulder from the Big Head Formation diamictite at Mount Arlington Heights. Sample locations, descriptions and complete geochemical data are reported in Table 1 and Appendix 1. Sampling protocol included the collection of approximately 2 kg of rock that was homogeneous, representative of the outcrop, and lacked veins and alteration. Samples were processed and analyzed at the Government of Newfoundland and Labrador geochemical laboratory. Sample preparation and analytical methods are outlined in Finch *et al.* (2018).

Rocks of the Avalon Terrane are known to have been affected by alteration and/or metasomatism (*e.g.*, Hughes and Malpas, 1971; Mills and Sandeman, 2015) and sporadic epidotization and hematitization throughout the Long Harbour–Placentia area (described above) suggest that many of the rocks in the study area are altered. This is corroborated by Large *et al.*'s (2001) box plot using alteration indices (Figure 4A). For this reason, high field strength (HFSE) and rare earth elements (REE), which are less sus-

ceptible to most fluid–rock alterations (*e.g.*, Pearce and Cann, 1973; Wood *et al.*, 1980; Middelburg *et al.*, 1988) are emphasized and more heavily relied upon for petrologic and tectonic interpretations.

ASSEMBLAGE 1: MAFIC ROCKS

Assemblage 1 includes two subsets. The mafic subset includes three basalt breccias. These are basalt, basaltic andesite and trachy-andesite (Le Maitre *et al.*, 1989; Figure 4B) based on their major-element compositions, and basalt based on their trace-element abundances (Pearce, 1996; Figure 4C). These rocks exhibit a wide range in major-element contents: *e.g.*, SiO_2 (42–53%), Mg# (40–63), CaO (3–8.9%). No iron enrichment trend is discernible within this small sample population (n=3). Trace-element contents also vary widely: *e.g.*, Zr (73–133 ppm), Cr (77–126 ppm), Ba (230–3069 ppm). The multi-element patterns of this subset are characterized by moderately steep slopes (mean La/Yb_{CN} = 4.5; Table 2), prominent Nb troughs (mean La/Nb_{CN} 5.2; Th/Nb_{CN} 8.9), and slightly negatively anomalous HFSEs (Figure 5). Relative to basaltic rocks of Assemblages 2 and 3, these have the highest (Th/La)_{CN}, (La/Nb)_{CN} and (Th/Nb)_{CN} ratios (Table 2). The mafic rocks of Assemblage 1 are moderately LREE- and Th-enriched, weakly calc-alkaline basalts through basaltic andesites (Figure 6A, B, D). In TiO₂/Yb vs. Nb/Yb space (Figure 6C), they mainly plot within the lower part of the mantle array, indicative of shallow melting and common among volcanic rocks from continental margins (Pearce, 2008). In Th/Yb vs. Nb/Yb space, they plot above the main mantle array, within the EMORB section of the volcanic arc array, owing to their elevated Th levels (Figure 6D), which indicate crustal/lithospheric contamination (Pearce, 2008).

ASSEMBLAGE 1: INTERMEDIATE ROCKS

The second subset of Assemblage 1 is mainly intermediate in composition (SiO_2 = 48–65%) and includes a crystal ash tuff, two crystal lithic tuffs and one lapilli tuff containing rhyolite fragments. They are mainly dacite and trachydacite, although one rock is a trachy-basalt, based on major-element compositions (Figure 4B). With the exception of one dacitic sample, they are andesite to basaltic andesite based on their trace-element compositions (Figure 4C). Relative to the basaltic Assemblage 1 rocks, these rocks have lower Mg#, Cr, Ni and V contents and higher Th and ΣREEs. Like the mafic rocks of Assemblage 1, the intermediate rocks also have relatively steep multi-element patterns (Figure 5) with pronounced Nb troughs and weakly negatively anomalous HFSEs. Relative to their mafic counterparts, the intermediate rocks have steeper multi-element slopes (average La/Yb_{CN} = 6.9), more pronounced P and Nb troughs and higher Th contents. These rocks are calc-alka-

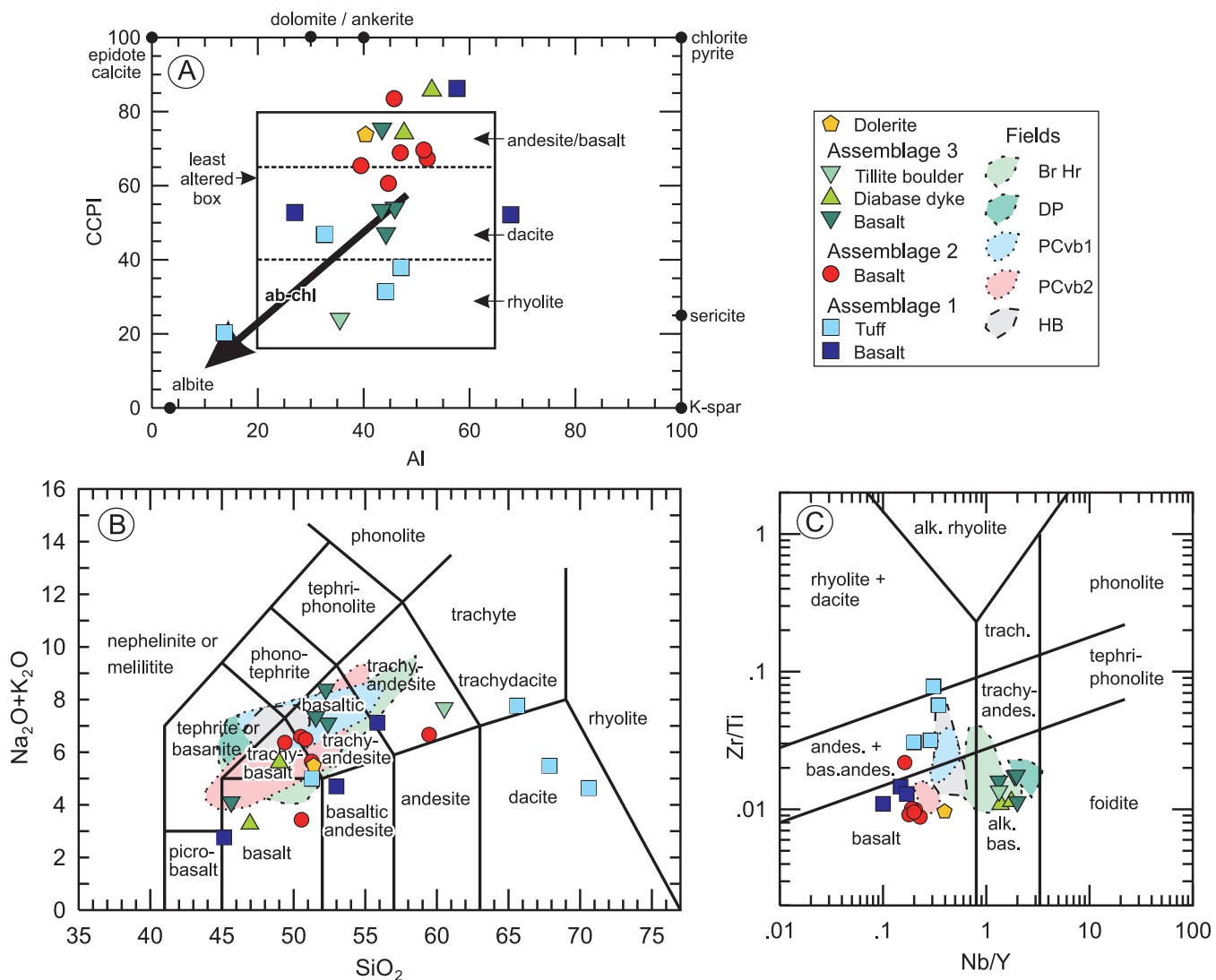


Figure 4. Rock classification diagrams showing the compositions of rocks from the Long Harbour–Placentia area. A) Alteration box-plot (Large et al., 2001); B) Based on major element content – silica vs. total alkalis silicate diagram normalized to 100% water free (after Le Maitre et al., 1989); C) Based on trace element content (after Pearce, 1996). Fields correspond to mafic rock assemblages from the Bonavista Peninsula (Mills and Sandeman, 2015). HB = calc-alkaline Headland basalt; PCvb2 = continental tholeiite series 2 of the Plate Cove volcanic belt; PCvb1 = continental tholeiite series 1 of the Plate Cove volcanic belt; DP = Dam Pond alkaline basalt; Br Hr = British Harbour alkaline basalt.

line (Figure 6A, B) and, as expected for silicic rocks, plot farther off the mantle array relative to the mafic rocks of Assemblage 1 (Figure 6C, D).

ASSEMBLAGE 2: THOLEIITES

Rocks of Assemblage 2 are basaltic trachy-andesite ($n=3$), basalt ($n=1$), trachy-basalt ($n=1$) and trachy-andesite ($n=1$) in terms of their major-element compositions (Figure 4B). They are all basaltic based on their trace-element compositions, with the exception of one andesite to basaltic andesite (Figure 4C). Assemblage 2 basalts have flatter

multi-element patterns [mean $(\text{La/Yb})_{\text{CN}} = 3.3$] and less pronounced Nb troughs [average $(\text{La/Nb})_{\text{CN}} = 2.7$; average $(\text{Th/Nb})_{\text{CN}} = 4.7$] than those of Assemblage 1 (Figure 5; Table 2). With one exception, these rocks lack Ti troughs, in contrast to the mafic rocks of Assemblage 1. The sample with a Ti trough also has considerably higher Th and lower P relative to the other five samples. This sample is more highly fractured, with epidote and chlorite veinlets, and patchy carbonate and chlorite dispersed throughout its groundmass, and is therefore more highly altered. Despite their moderate Nb troughs, consistent with an apparent calc-alkaline affinity (Figures 5 and 6A), these rocks are transi-

tional (Figure 6B), as indicated by their flatter multi-element patterns (Figure 5) and typically subdued Nb troughs [lower $(\text{La}/\text{Nb})_{\text{CN}}$ and $(\text{Th}/\text{Nb})_{\text{CN}}$ relative to Assemblage 1 rocks (Table 2)]. In TiO_2/Yb vs. Nb/Yb space (Pearce, 2008), they plot on the EMORB side of the mantle array (Figure 6C) and, like the Assemblage 1 basalts, Assemblage 2 basalts plot above, albeit closer to the mantle array in Th/Yb vs. Nb/Yb space (Figure 6D).

ASSEMBLAGE 3: ALKALINE BASALTS

Assemblage 3 basalts are basalt, trachy-basalt, basaltic trachy-andesite and trachy-andesite based on their major-element compositions (Figure 4B), and alkali basalt based on their trace elements (Figure 4C). These basalts have the steepest multi-element slopes (mean $(\text{La}/\text{Yb})_{\text{CN}} = 10.9$) of the three basaltic assemblages (Figure 5). They also have the highest Mg# and V, Cr and Ni contents of all three assemblages (Table 2). Their steep multi-element patterns lack Nb and Ti troughs, and exhibit very minor dips in Hf and Zr (Figure 5). In La–Y–Nb space (Figure 6A), these rocks straddle the continental and intercontinental rift (alkaline) fields. In both TiO_2/Yb vs. Nb/Yb and Th/Yb vs. Nb/Yb space, Assemblage 3 rocks plot close to OIB along the mantle array (Figure 6C, D).

Table 2. Summary of salient lithogeochemical features of volcanic assemblages from the Long Harbour–Placentia area

	Assemblage 1 Mafics	Assemblage 2 Intermediates	Assemblage 3
SiO_2	42-53	48-65	47-58
$(\text{La}/\text{Yb})_{\text{CN}}$	4.5	6.9	3.3
$(\text{La}/\text{Sm})_{\text{CN}}$	1.9	2.5	1.7
$(\text{Gd}/\text{Yb})_{\text{CN}}$	1.7	1.7	1.6
$(\text{Th}/\text{La})_{\text{CN}}$	1.8	2.8	1.6
$(\text{La}/\text{Nb})_{\text{CN}}$	5.2	4.0	2.7
$(\text{Th}/\text{Nb})_{\text{CN}}$	8.9	10.4	4.7
Eu/Eu^* Range	.94-1.03	.79-.86	0.78-1.89
Th	2.3-3.7	7.4-12.3	1.0-7
Sr	287-381	37-1406	161-363
Zr	73-133	162-224	72-102
ΣREE	71-126	132-265	61-90
Mg#	40-63	10-43	48-58
TiO_2	1.1-1.5	0.5-0.9	0.7-1.8
V	106-282	48-137	173-351
Cr	77-126	6-22	82-155
Ni	24-90	8-28	32-83
Sc	32-45	10-23	28-41
			13-28

Note: Mg# = [molecular $\text{MgO}/(\text{MgO} + \text{FeOT})$]*100; subscript CN = chondrite normalized; ΣREE = sum of rare earth elements. All values cited are the mean for each assemblage

ARGENTIA DOLERITE

As the margins of the Argentia dolerite are not exposed, its host rock could not be established in the field, and therefore its relative timing of emplacement cannot be ascertained. Chemically, it is classified as trachy-basalt based on its major-element composition, and as basalt based on its trace-element content (Figure 4B, C). Its multi-element pattern is flatter than that of any other rock from the study area ($\text{La}/\text{Yb})_{\text{CN}} = 2.2$, showing minor LREE enrichment and no notable negative anomalies in the HFSEs (Figure 5). The dolerite is EMORB-like, and plots close to EMORB on most discrimination diagrams (Figure 6A, C, D).

DISCUSSION

INTERPRETATION AND IMPLICATIONS OF DIAMICTITES IN THE LONG HARBOUR AREA

Brückner's (1977) tillite reportedly outcrops farther upsection (at the top of the hill) relative to the diamictites examined in the current investigation. The diamictites of the Big Head Formation, described here, may have originated in a peri-glacial environment (see below). However, nonglacial depositional processes can also produce unsorted sediments that resemble glacial products (Carte and Eyles, 2012a, b). For example, King (1990) interpreted a mixtite unit within the Conception Group on northeastern Avalon Peninsula to be volcanogenic in origin, despite similarities in lithology and stratigraphic position that led Hsu (1978) to interpret the same mixtite unit as a "tilloid" correlative to the Gaskiers Formation on southern Avalon Peninsula. Volcanogenic deposits, however, should compositionally reflect the volcanic source, resulting in a largely monolithic clast composition. At Mount Arlington, the basalt clast-rich horizon lying between maroon mudstone–grey sandstone facies and overlying grey laminated mudstone ± sandstone facies is largely monolithic and possibly volcanogenic. The majority of all Mount Arlington Heights and Long Harbour diamictites, however, are polyolithic, reflecting mixed provenance, which is more consistent with a glacial origin (Arnaud and Etienne, 2011). As is true for the Trinity facies on Bonavista Peninsula, the Long Harbour diamictites are commonly volcaniclastic, as a high proportion of the contained clasts are volcanic, but siliciclastic clasts ranging from chert to sandstone are also represented indicating a

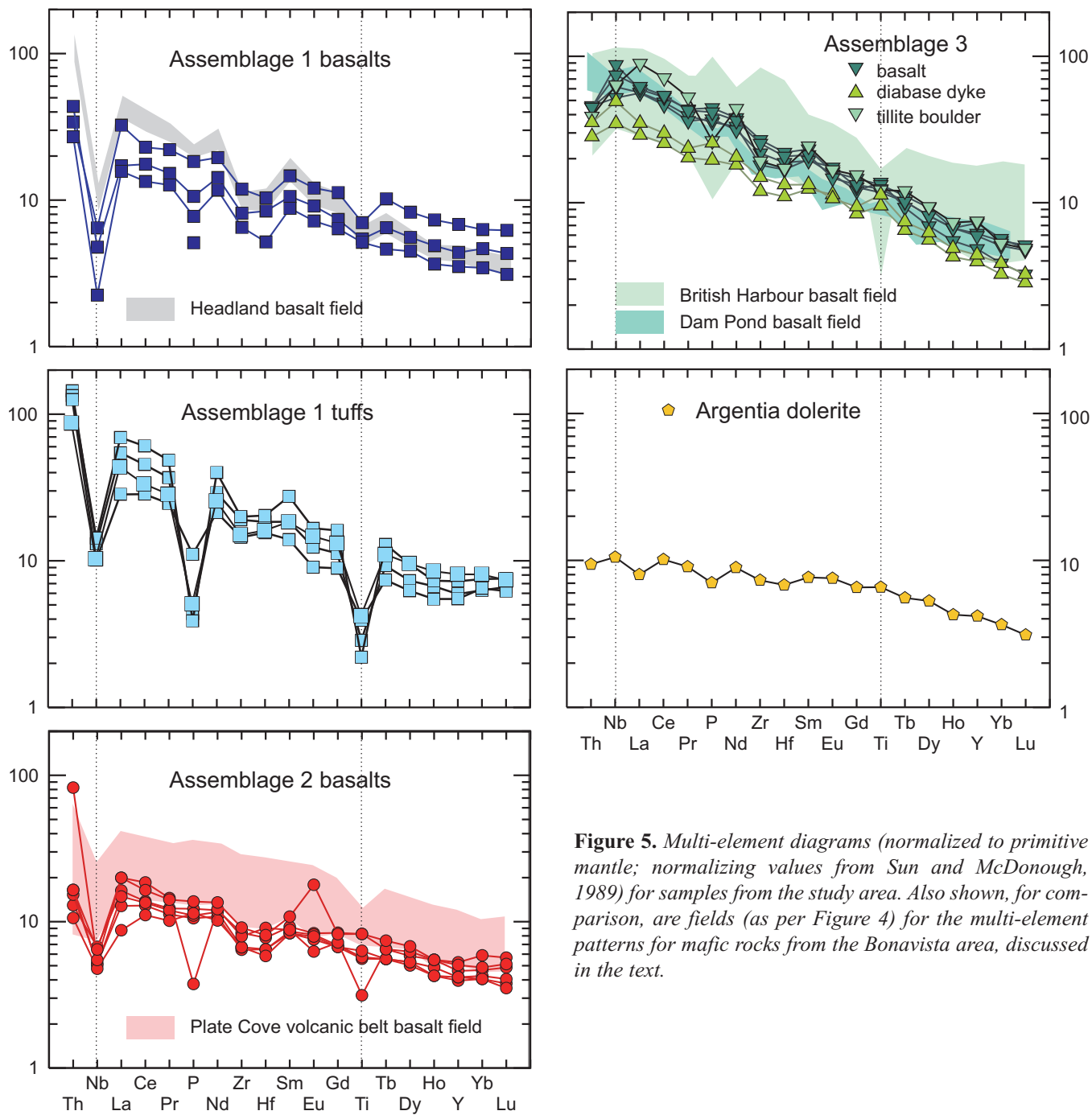


Figure 5. Multi-element diagrams (normalized to primitive mantle; normalizing values from Sun and McDonough, 1989) for samples from the study area. Also shown, for comparison, are fields (as per Figure 4) for the multi-element patterns for mafic rocks from the Bonavista area, discussed in the text.

broad provenance that is not restricted to local volcanic sources. Bent and ruptured laminae (e.g., Plate 4A) are consistent with a dropstone interpretation. Although projectile volcanic detritus can result in the deflection and penetration of laminae (Bennett *et al.*, 1996), none of the observed clasts resemble the fusiform, spindle, or almond shape characteristic of pyroclastic materials. Instead, clast shapes range from rounded to angular, including faceted, bullet-shaped and flat-iron clasts (Plate 4A). These clast mor-

phologies are consistent with dropstone rainout from a rafted-ice source (e.g., Benn and Evans, 1998; Arnaud and Etienne, 2011).

Mass transport processes, such as deep marine gravity flows (particularly at extensional margins), have been interpreted as the depositional mechanism for diamictite deposits that were previously interpreted to be glacial (e.g., King, 1990; Carto and Eyles, 2012a, b; Arnaud and Eyles, 2002).

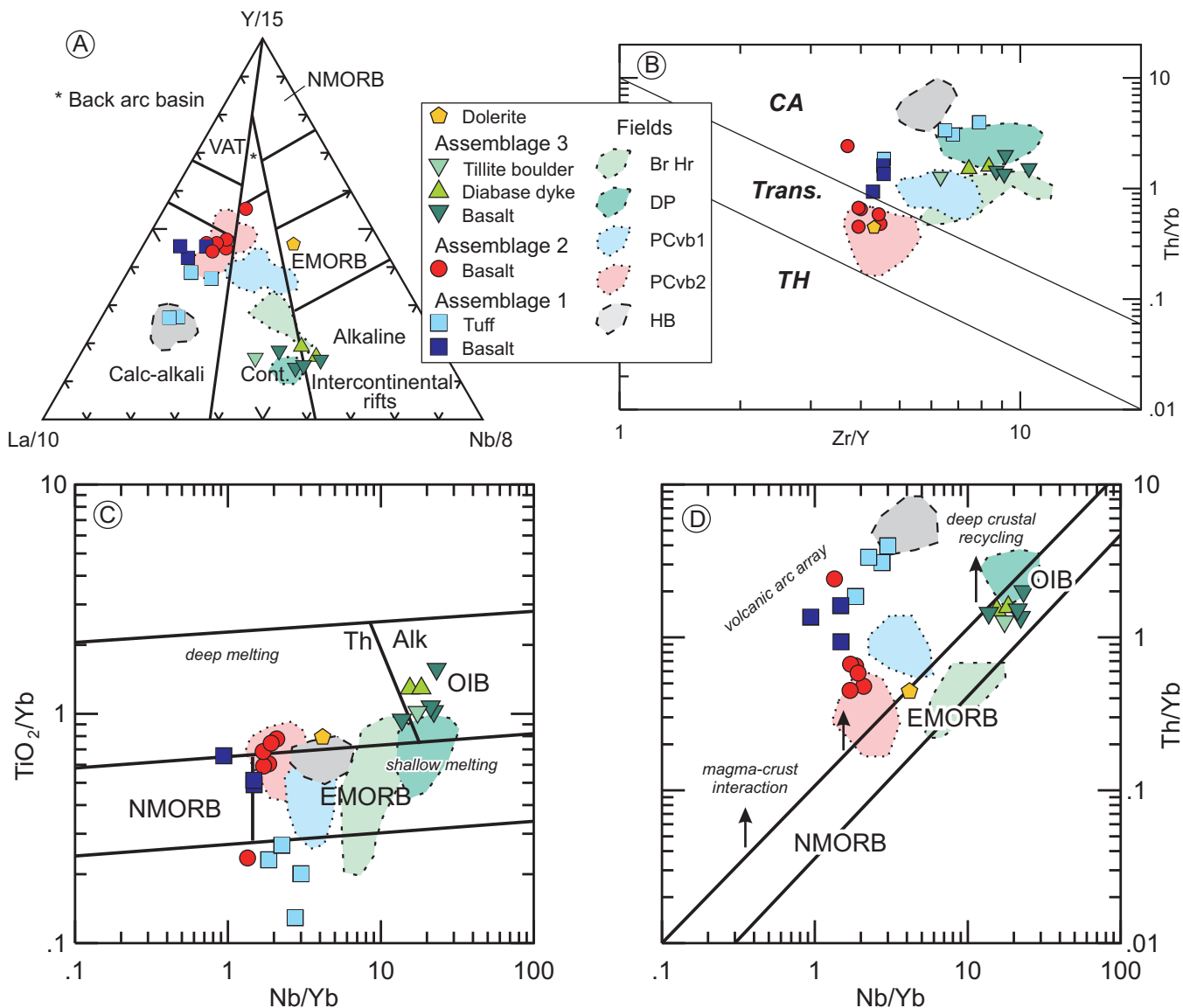


Figure 6. Tectonic discrimination diagrams for samples from the study area. A) Ternary plot of $\text{La}/\text{Nb}-\text{Y}$ (after Cabanis and Lécollé, 1989); B) Logarithmic plot of Th/Yb vs. Zr/Y (after Ross and Bédard, 2009); C) Melting depth proxy, TiO_2/Yb vs. Nb/Yb (after Pearce, 2008); D) Crustal input proxy, Th/Yb vs. Nb/Yb (after Pearce, 2008).

Matrix-supported, unsorted conglomerates, clastic dykes, and slump folds ranging from recumbent to sheath-like, are not unique to glacial deposits, and are common in debrites or olistostromes (e.g., Tohver *et al.*, 2018). It is therefore possible that some of the facies described from the study area may have been redeposited by mass-transport processes, but the faceted, bullet-shaped and flat-iron clast morphologies are nevertheless consistent with a glacial origin that could have been affected by nominal subsequent transport, permitting preservation of these distinctive clast shapes. The truncation of mudstone laminae by overlying planar laminated mudstone results in common dislocation surfaces (e.g., Plate 3A) that closely resemble glaciogenic dislocations,

which are interpreted to form as fragments of semi-consolidated (or frozen) underlying strata were rotated or plucked by the deforming overlying sediment (Chumakov, 2015). Similar features can also form in a slope environment, and are therefore not diagnostic of a glacial setting. The faceted, bullet-shaped and flat-iron clasts, the deformation and local penetration of lamellae by oversized clasts, interpreted as dropstones, and lithological and stratigraphic similarities between diamictites in the Big Head Formation at Long Harbour, and those of the Trinity facies rocks on Bonavista (see Plate 7 of Normore, 2011), lead the authors to concur with Brückner's (1977) interpretation of a glaciogenic origin for these rocks. Correlation with the ca. 580 Ma

Trinity and Gaskiers diamictites is proposed but remains to be unequivocably established.

REGIONAL STRATIGRAPHIC IMPLICATIONS OF DIAMICTITES IN THE LONG HARBOUR AREA

Whether the diamictites in the study area were deposited directly by glacial/deglacial processes or were (re)deposited by mass-flow processes, their lithology and facies associations bear striking resemblance to diamictites of the glacial Trinity facies on Bonavista Peninsula (Normore, 2011; Pu *et al.*, 2016). If these glaciogenic units are correlative, then King's (1988) designation as Big Head Formation, for siliciclastic rocks stratigraphically above the Gibbett Hill Formation (Signal Hill Group) on the Bay de Verde sub-peninsula, becomes problematic (*see* Figure 2). Although there are no age constraints on the Gibbett Hill Formation, the Signal Hill Group is interpreted to conformably and gradationally overlie the St. John's Group (King, 1990), which in turn conformably overlies the Conception Group. U–Pb (zircon) age constraints from southern Avalon Peninsula include 565 ± 3 Ma (Benus, 1988), 566.25 ± 0.35 Ma (Canfield *et al.*, 2020), and 565.00 ± 0.16 Ma (Matthews *et al.*, 2020) for the Mistaken Point Formation (upper Conception Group) and 562.5 ± 1.1 Ma for lower St. John's Formation rocks (Canfield *et al.*, 2020). The Gibbett Hill Formation is therefore expected to be younger than *ca.* 562 Ma. If the Big Head Formation diamictites at Long Harbour are correlative to the Trinity facies and Gaskiers Formation, then either the rocks on Bay de Verde sub-peninsula assigned to Gibbett Hill Formation are not correlative to those on eastern Avalon Peninsula, or rocks of the Big Head Formation unit on Bay de Verde are not correlative to the unit defined at its type locality at Long Harbour (*see* Figure 2). Possibly, significant thrust emplacement, hitherto unrecognized, could be invoked to place the older Big Head Formation rocks above the younger Gibbett Hill Formation rocks at Bay de Verde. As such structural imbrication is unlikely to be restricted to the interface between these two units, this interpretation is considered unlikely. It is more probable that the lithostratigraphic designation of either Gibbett Hill Formation or Big Head Formation on the Cape de Verde peninsula (or both) is incorrect.

INTERPRETATION AND IMPLICATIONS OF BULL ARM FORMATION VOLCANIC ROCKS

Mafic and intermediate rocks of Assemblage 1 are weakly calc-alkaline, and are less LREE- and LILE-enriched than the Headland basalt from the Bonavista Peninsula (*see* Figures 5 and 6A, B). Assemblage 1 mafic rocks have lower $(\text{La}/\text{Yb})_{\text{CN}}$ ratios and Th contents than the Headland basalt (Figures 5 and 6A, B, D). The mafic rocks of Assemblage 1 are spatially restricted to north of Ship

Harbour, on the north side of the southwest projection of the Ship Harbour fault (Figure 3). One Assemblage 1 tuff from northeast of Placentia overlies tholeiitic flows of Assemblage 2. However, this sample is a crystal lithic tuff that contains siltstone and other lithic fragments (Table 1), so that its whole-rock chemistry is a mix of pyroclastic and epiclastic material and not representative of the magma source. This is also likely the case for the other tuffs of Assemblage 1. Based on Pearce's (2008) use of Ti–Yb ratio as a proxy for melting depth, the calc-alkaline Assemblage 1 basalts were likely derived from an undepleted, shallow asthenospheric source (Figure 6C). Their relatively high Th/Yb ratios, a proxy for subduction zone influence or crustal input (Pearce, 2008), indicates their mantle source was modified by supra-subduction zone-derived fluids/magma (Figure 6D). Assemblage 1 basalts are similar to the calc-alkaline basalts from the Bonavista area, albeit less LREE- and Th-enriched (Figure 6A, B, D).

Assemblage 2 basalts are chemically similar to one of the two tholeiitic basalt series (PCvb2 of Mills and Sandeman, 2015) identified within the Plate Cove volcanic belt on the Bonavista Peninsula (*see* Figures 5 and 6). Basalts of the Plate Cove volcanic belt are intercalated with silicic tuffaceous rocks locally dated at *ca.* 592 and 591 Ma (Mills *et al.*, 2016), providing strong evidence that tholeiitic volcanism followed calc-alkaline volcanism in the Bonavista area. According to Pearce's (2008) Ti–Yb proxy for melting depth, Assemblage 2 basalts were derived from a weakly enriched, slightly deeper source than that of Assemblage 1 rocks (Figure 6C). Based on their lower Th/Yb ratios relative to Assemblage 1 mafic rocks, the source of Assemblage 2 rocks had either a reduced supra-subduction zone metasomatic modification, and/or involved less lithospheric recycling in the petrogenesis of its parental magma (Figure 6D). Based on our limited sampling, Assemblage 2 basalts are apparently spatially restricted to the Bull Arm Formation anticline south of the Ship Harbour fault (Figure 3).

Assemblage 3 basalts are alkaline (Figures 4B, 5 and 6) and occur near the top of the Bull Arm Formation in the study area (Figure 3). North of Placentia, two dykes having alkaline chemistry (Assemblage 3) crosscut tholeiitic basalts of Assemblage 2 (Figure 6E), demonstrating that Assemblage 3 rocks are younger. The alkaline flow at Ship Harbour is at the top of the Bull Arm Formation and overlies calc-alkaline Assemblage 1 rocks, indicating that Assemblage 3 is younger than Assemblage 1. In addition, the basalt boulder sampled from the tillite within the Big Head Formation (Figure 3) is also alkaline, indicating that alkaline magmatism preceded the deposition of the diamictite. It is possible that some alkaline mafic magmatism was concomitant with deglaciation in the Long Harbour area, but further

studies of the basalt clast-rich horizon between maroon mudstone facies and overlying grey laminated mudstone facies are required to definitively confirm this proposal.

Crosscutting relationships and superposition clearly show that emplacement of Assemblage 3 postdates that of Assemblages 1 and 2. The relative timing of Assemblages 1 and 2 cannot be firmly established based on this reconnaissance investigation. Based on age and petrochemistry constraints on Bull Arm Formation rocks at the Isthmus of Avalon, Eastport and Bonavista areas (*see* ‘Age and Chemical Constraints on the Bull Arm Formation’), the same trend is expected for Bull Arm Formation rocks in the Long Harbour–Placentia area – *i.e.*, calc-alkaline magmatism preceded tholeiitic (and/or transitional magmatism), which was, in turn, followed by alkaline magmatism. Further mapping, geochronological, and lithogeochemical studies are recommended for the southwestern Avalon Peninsula, targeting the felsic core of the Cape St. Mary’s sub-peninsula (*see* Figures 1 and 3), in particular.

On the Bonavista Peninsula, the timing of alkaline magmatism relative to the *ca.* 580 Ma deglaciation event (Pu *et al.*, 2016) is apparently diachronous. On the northeast part of the Peninsula, the alkaline Dam Pond basalts (Mills and Sandeman, 2015) occupy a structural culmination or dome flanked by rocks that include the Trinity diamictite. On the southwestern part of the Peninsula, however, alkaline fragmental basalt locally overlies the Trinity diamictite, with approximately 50 m of intervening fine-grained siliciclastic strata (*see also* Pu *et al.*, 2016). Farther south, at British Harbour, alkaline basalts occur within an upward-coarsening sequence (Rocky Harbour Formation) near the transition to coarse-grained, terrestrial red beds of the Crown Hill Formation, uppermost Musgravetown Group (Mills and Sandeman, unpublished data; *see also* Normore, 2012a, b). The timing of this transition is not constrained. Apparent diachronous emplacement of alkaline basalts on the Bonavista Peninsula suggests the possibility of a protracted period of alkaline volcanism during the Ediacaran in the Avalon Terrane. The stratigraphic position of alkaline basalts almost immediately below diamictites in both the Long Harbour area and on northeastern Bonavista Peninsula (Dam Pond; *see* Figure 1) further raises the question of whether this magmatism provided a heat source that contributed to widespread deglaciation of an area covering at least 250 x 200 km in the Avalon Terrane in Newfoundland (*see also* Brückner and Anderson, 1971). Subglacial volcanism has provided sufficient heat to induce melting beneath the Pine Island Glacier of the West Antarctic Ice Sheet (Loose *et al.*, 2018; *see also* Smellie and Skilling, 1994) and a link between *ca.* 580-Ma magmatism and the globally recognized Gaskiers event has previously been proposed (Youbi *et al.*, 2020).

Recommended future work should include age constraints for the diamictite in the Long Harbour area and targeted studies to better understand the lithostratigraphy of the Musgravetown Group, particularly on the Bay de Verde sub-peninsula. Age and petrochemical constraints are also required for other parts of the Bull Arm Formation including the felsic dome south of the current study area, mafic and felsic units north and south of Bull Arm, and the two north-trending Love Cove schist units south of the Eastport area (Figure 1). Detailed sedimentological and stratigraphic studies of McCartney’s (1967) Snows Pond/Whiteway and Big Head formations are recommended to resolve possible erroneous litho-correlations that were retained in King’s (1988) compilation for Avalon Peninsula. Additionally, northeast-trending faults, such as the Ship Harbour fault (Figure 3), should be investigated to determine the nature and magnitude of offset.

ACKNOWLEDGMENTS

The first author acknowledges the sound field assistance of Ofure Onodenalore and discussions in the field with visiting scientists Phil McCausland (Western University), and Boris Robert, Mathew Domeier and Hans Jørgen Kjøll (University of Oslo) during the 2019 field season. The second author thanks Cody Spurrell for solid field assistance in 2017. We thank Chris Finch and the Geological Survey Branch’s laboratory team for timely delivery of quality lithogeochemical data. Kim Morgan of the Department of Industry, Energy and Technology drafted the map figures. Critical reviews by Dr. David Lowe and Dr. Alana Hinchee helped to improve the manuscript. The manuscript was typeset by Joanne Rooney.

REFERENCES

- Arnaud, E. and Etienne, J.L.
2011: Recognition of glacial influence in Neoproterozoic sedimentary successions (Chapter 3). *In* The Geological Record of Neoproterozoic Glaciations. Edited by E. Arnaud, G.P. Halverson and G. Shields-Zhou. Geological Society, London, Memoirs, Volume 36, pages 39–50.
- Arnaud, E. and Eyles, C.H.
2002: Glacial influence on Neoproterozoic sedimentation: the Smalfjord Formation, northern Norway. *Sedimentology*, Volume 49, pages 765–788.
- Benn, D.I. and Evans, D.J.A.
1998: Glaciers and Glaciation. Hodder Education, London. ISBN-10: 0340584319; ISBN-13: 9780340584316; 734 pages.

- Bennett, M.R., Doyle, P. and Mather, A.E.
1996: Dropstones: their origin and significance. *Palaeogeography, Palaeoclimatology, Palaeoecology*, Volume 121, pages 331-339.
- Benus, A.P.
1988: Sedimentological context of a deep-water Ediacaran fauna (Mistaken Point, Avalon Zone, eastern Newfoundland). In *Trace Fossils, Small Shelly Fossils and the Precambrian-Cambrian Boundary*. Edited by E. Landing, G.M. Narbonne and P. Myrow. The University of the State of New York, Bulletin 463, pages 8-9.
- Boulton, G.S.
1978: Boulder shapes and grain-size distributions of debris as indicators of transport paths through a glacier and till genesis. *Sedimentology*, Volume 25, pages 773-799.
- Brückner, D.
1977: Significance of new tillite finds for east-west correlation of Proterozoic Avalon-zone formations in southeastern Newfoundland (Canada). *Estud. Geology*, Volume 33, pages 95-102.
- Brückner, D. and Anderson, M.M.
1971: Late Precambrian glacial deposits in southeastern Newfoundland, a preliminary note. *Geological Association of Canada Proceedings*, Volume 24, pages 95-12.
- Buddington, A.F.
1919: Reconnaissance of the Algonkian rocks of southeastern Newfoundland. *Geological Society of America Bulletin*, Volume 25, 40 pages.
- Cabanis, B. and Lecolle, M.
1989: Le diagramme La/10-Y/15-Nb/8: un outil pour la discrimination des séries volcaniques et la mise en évidence des processus de mélange et/ou de contamination crustale. *Comptes Rendus de l'Académie des Sciences, Series II*, Volume 309, pages 2023-2029.
- Canfield, D.E., Knoll, A.H., Poulton, S.W., Narbonne, G.M. and Dunning, G.R.
2020: Carbon isotopes in clastic rocks and the Neoproterozoic carbon cycle. *American Journal of Science*, Volume 320, pages 97-124. DOI: 10.2475/02.2020.01
- Carte, S.L. and Eyles, N.
2012a: Identifying glacial influences on sedimentation in tectonically-active, mass flow dominated arc basins with reference to the Neoproterozoic Gaskiers glaciation (c. 580 Ma) of the Avalonian-Cadomian Orogenic Belt. *Sedimentary Geology*, Volume 261-262, pages 1-14.
- 2012b: Sedimentology of the Neoproterozoic (c. 580 Ma) Squantum 'Tillite', Boston Basin, USA: Mass flow deposition in a deep-water arc basin lacking direct glacial influence. *Sedimentary Geology*, Volume 269, pages 1-14.
- Christie, A.M.
1950: Geology of Bonavista map-area, Newfoundland (summary account). Department of Mines and Technical Surveys. Geological Survey of Canada. Paper 50-7, 40 pages [002C/0007].
- Chumakov, N.M.
2015: Problem of the identification of ancient glacial sediments. *Lithology and Mineral Resources*, Volume 50, No. 2, pages 148-158.
- Colman-Sadd, S.P., Hayes, J.P. and Knight, I.
1990: Geology of the Island of Newfoundland (digital version of Map 90-01); Scale: 1:1 000 000. Government of Newfoundland and Labrador, Department of Mines and Energy, Geological Survey Branch, Open File NFLD/2192.
- Dec, T., O'Brien, S.J. and Knight, I.
1992: Late Precambrian volcaniclastic deposits of the Avalonian Eastport basin (Newfoundland Appalachians): petrofacies, detrital clinopyroxene and paleotectonic implications. *Precambrian Research*, Volume 59, pages 243-262.
- Finch, C., Roldan, R., Walsh, L., Kelly, J. and Amor, S.
2018: Analytical methods for chemical analysis of geological materials. Government of Newfoundland and Labrador, Department of Natural Resources, Geological Survey, Open File NFLD/3316, 67 pages.
- Hambrey, M.J. and Glasser, N.F.
2012: Discriminating glacier thermal and dynamic regimes in the sedimentary record. *Sedimentary Geology*, Volume 251-252, pages 1-33. DOI: 10.1016/j.sedgeo.2012.01.008
- Hayes, A.O.
1948: Geology of the area between Bonavista and Trinity bays, eastern Newfoundland. Geological Survey of Newfoundland, Bulletin 32 (part 1), pages 1-37.
- Howell, B.F.
1920: The Middle Cambrian of Newfoundland, and their relations. *Science, New Series*, Volume 51, Number 1330.

- Hsu, E.
1978: Geology of the St. John's Peninsula (1N/10 and 1N/15); Pouch Cove - St. John's, Newfoundland. Government of Newfoundland and Labrador, Department of Mines and Energy, Mineral Development Division, Map 7836.
- Hughes, C.J. and Malpas, J.G.
1971: Metasomatism in the late Precambrian Bull Arm Formation in southeastern Newfoundland: recognition and implications. The Geological Association of Canada, Proceedings, Volume 24, Number 1, pages 85-93.
- Israel, S.
1998: Geochronological, structural and stratigraphic investigation of a Precambrian unconformity between the Harbour Main Group and Conception Group, east coast Holyrood Bay, Avalon Peninsula, Newfoundland. Unpublished B.Sc. (Honours) thesis, Memorial University of Newfoundland, 78 pages.
- Jenness, S.E.
1963: Terra Nova and Bonavista map-areas, Newfoundland (2D E ½ and 2C). Geological Survey of Canada, Memoir 327, 184 pages.
- King, A.F.
1988: Geology of the Avalon Peninsula, Newfoundland (parts of 1K, 1L, 1M, 1N and 2C). Government of Newfoundland and Labrador, Department of Mines, Mineral Development Division, Map 88-01.
1990: Geology of the St. John's area. Government of Newfoundland Labrador, Department of Mines and Energy, Geological Survey Branch, Report 90-2, pages 1-92.
- Knight, I. and O'Brien, S.J.
1988: Stratigraphy and sedimentology of the Connecting Point Group and related rocks, Bonavista Bay, Newfoundland: An example of a Late Precambrian Avalonian basin. *In Current Research*. Government of Newfoundland and Labrador, Department of Mines, Mineral Development Division, Report 88-1, pages 207-228.
- Large, R.R., Gemmell, J.B., Paulick, H. and Huston, D.L.
2001: The alteration box plot: a simple approach to understanding the relationships between alteration mineralogy and lithogeochemistry associated with VHMS deposits. *Economic Geology*, Volume 96, pages 957-971.
- Le Maitre, R.W., Bateman, P., Dudek, A.J. and Keller, M.J.
1989: A Classification of Igneous Rocks and Glossary of Terms. Oxford, Blackwell. 193 pages.
- Loose, B., Naveira Garabato, A.C., Schlosser, P., Jenkins, W.J., Vaughan, D. and Heywood, K.J.
2018: Evidence of an active volcanic heat source beneath the Pine Island Glacier. *Nature Communications*. DOI: 10.1038/s41467-018-04421-3
- Matthews, J.J., Liu, A.G., Yang, C., McIlroy, D., Levell, B. and Condon, D.J.
2020: A chronostratigraphic framework for the rise of the Ediacaran macrobiota: new constraints from Mistaken Point Ecological Reserve, Newfoundland. Geological Society of America. DOI: 10.1130/B35646.1, 13 pages.
- McCartney, W.D.
1956: Argentia, Newfoundland. Geological Survey of Canada, Preliminary Map 55-11.
1967: Whitbourne map area, Newfoundland, Geological Survey of Canada, Memoir 341, 135 pages.
- Middelburg, J.J., Van der Weijden, C.H. and Woittiez, J.R.W.
1988: Chemical processes affecting the mobility of major, minor and trace elements during weathering of granitic rocks. *Chemical Geology*, Volume 68, pages 253-273.
- Mills, A.J.
2014: Preliminary results from bedrock mapping in the Sweet Bay area (parts of NTS map areas 2C/5 and 2C/12), western Bonavista Peninsula, Newfoundland. *In Current Research*. Government of Newfoundland and Labrador, Department of Natural Resources, Geological Survey, Report 14-1, pages 135-154.
- Mills, A.J., Dunning, G.R. and Langille, A.
2016: New geochronological constraints on the Connecting Point Group, Bonavista Peninsula, Avalon Zone, Newfoundland. *In Current Research*. Government of Newfoundland and Labrador, Department of Natural Resources, Geological Survey, Report 16-1, pages 153-171.
- Mills, A.J., Dunning, G.R., Murphy, M. and Langille, A.
2017: New geochronological constraints on the timing of magmatism for the Bull Arm Formation, Musgravetown Group, Avalon Terrane, Newfoundland.

- In Current Research.* Government of Newfoundland and Labrador, Department of Natural Resources, Geological Survey, Report 17-1, pages 1-17.
- Mills, A.J., Dunning, G.R. and Sandeman, H.A.I.
2020: Lithogeochemical, isotopic and U-Pb (zircon) age constraints on arc- to rift-magmatism, northwestern and central Avalon Terrane, Newfoundland: Implications for local stratigraphy. *Canadian Journal of Earth Sciences.* DOI: 10.1139/cjes-2019-0196.
- Mills, A.J. and Sandeman, H.A.I.
2015: Preliminary lithogeochemistry for mafic volcanic rocks from the Bonavista Peninsula, northeastern Newfoundland. *In Current Research.* Government of Newfoundland and Labrador, Department of Natural Resources, Geological Survey, Report 15-1, pages 173-189.
- Normore, L.S.
2011: Preliminary findings on the geology of the Trinity map area (NTS 2C/06), Newfoundland. *In Current Research.* Government of Newfoundland and Labrador, Department of Natural Resources, Geological Survey, Report 11-1, pages 273-293.
- 2012a: Geology of the Random Island map area (NTS 2C/04), Newfoundland. *In Current Research.* Government of Newfoundland and Labrador, Department of Natural Resources, Geological Survey, Report 12-1, pages 121-145.
- 2012b: Geology of the Random Island map area (NTS 2C/04), Newfoundland. Map 2012-06, Scale 1:50 000. Government of Newfoundland and Labrador, Department of Natural Resources, Geological Survey, Open File 002C/04/0191.
- O'Brien, S.J., Dunning, G.R., Dubé, C.F., Sparkes, B., Israel, S. and Ketchum, J.
2001: New insights into the Neoproterozoic geology of the central Avalon Peninsula (parts of NTS map areas 1N/6, 1N/7 and 1N/3), eastern Newfoundland. *In Current Research.* Government of Newfoundland and Labrador, Department of Mines and Energy, Geological Survey, Report 2001-1, pages 169-189.
- O'Brien, S.J. and King, A.F.
2004: Late Neoproterozoic to earliest Paleozoic stratigraphy of the Avalon Zone in the Bonavista Peninsula, Newfoundland: An update. *In Current Research.* Government of Newfoundland and Labrador, Department of Mines and Energy, Geological Survey, Report 04-1, pages 213-224.
- O'Brien, S.J., O'Brien, B.H., Dunning, G.R. and Tucker, R.D.
1996: Late Neoproterozoic Avalonian and related peri-Gondwanan rocks of the Newfoundland Appalachians. *In Avalonian and Related Peri-Gondwanan Terranes of the Circum-North Atlantic,* Boulder, Colorado. Edited by R.D. Nance and M.D. Thompson. Geological Society of America, Special Paper 304.
- Pearce, J.A.
1996: A user's guide to basalt discrimination diagrams. *In Trace Element Geochemistry of Volcanic Rocks; Applications for Massive Sulphide Exploration.* Short Course Notes, Geological Association of Canada, Volume 12, pages 79-113.
- 2008: Geochemical fingerprinting of oceanic basalts with applications to ophiolite classification and the search for Archean oceanic crust. *Lithos,* Volume 100, pages 14-48.
- Pearce, J.A. and Cann, J.R.
1973: Tectonic setting of basic volcanic rocks determined using trace element analyses. *Earth and Planetary Science Letters,* Volume 19, pages 290-300.
- Pu, J.P., Bowring, S.A., Ramezani, J., Myrow, P., Raub, T.D., Landing, E., Mills, A., Hodgin, E. and Macdonald, F.A.
2016: Dodging snowballs: Geochronology of the Gaskiers glaciation and the first appearance of the Ediacaran biota. *Geology.* Geological Society of America, Data Repository item 2016326; DOI: 10.1130/G38284.1, 4 pages.
- Rose, E.R.
1952: Torbay map-area, Newfoundland. Geological Survey of Canada, Memoir 265.
- Ross, P.-S. and Bédard, J.H.
2009: Magmatic affinity of modern and ancient subalkaline volcanic rocks determined from trace-element discriminant diagrams. *Canadian Journal of Earth Sciences,* Volume 46, pages 823-839.
- Skipton, D.R., Dunning, G.R. and Sparkes, G.W.
2013: Late Neoproterozoic arc-related magmatism in the Horse Cove Complex, eastern Avalon Zone, Newfoundland. *Canadian Journal of Earth Sciences,* Volume 50, pages 462-482.
- Smellie, J.L. and Skilling, I.P.
1994: Products of subglacial volcanic eruptions under different ice thicknesses: two examples from Antarctica. *Sedimentary Geology,* Volume 91, pages 115-129.

- Sun, S.S. and McDonough, W.F.
1989: Chemical and isotopic systematics of oceanic basalts: implications for mantle composition and processes. *In* Magmatism in the Ocean Basin. Edited by A.D. Saunders and M.J. Norry. Geological Society of London, Special Publication 42, pages 313-345.
- Tohver, E., Schmieder, M., Lana, C., Mendes, P.S.T., Jourdan, F., Warren, L. and Riccomini, C.
2018: End-Permian impactogenic earthquake and tsunami deposits in the intracratonic Paraná Basin or Brazil. Geological Society of America, Volume 130, Issue 7-8, pages 1099-1120.
- Widmer, K.
1949: Unpublished map and incomplete report on the Glovertown–Clode Sound area. Geological Survey of Newfoundland. [2D9/65]
- Williams, H. and King, A.F.
1979: Trepassey map area, Newfoundland. Geological Survey of Canada, Memoir 389, 24 pages.
- Wood, D.A.
1980: The application of a Th-Hf-Ta diagram to problems of tectomagmatic classification and to establishing the nature of crustal contamination of basaltic lavas of the British Tertiary Volcanic Province. Earth and Planetary Science Letters, Volume 50, pages 11-30.
- Youbi, N., Ernst, R.E., Söderlund, Ulf, Boumehdi, M.A., Lahna, A.A., Tassinari, C.C.G., Moume, W.E. and Bensalah, M.K.
2020: The Central Iapetus magmatic province: an updated review and link with the ca. 580 Ma Gaskiers glaciation. *In* Mass Extinctions, Volcanism, and Impacts: New Developments. Edited by T. Adatte, D.P.G. Bond and G. Keller. Geological Society of America, Special Paper 544, pages 35-66. [https://doi.org/10.1130/2020.2544\(02\)](https://doi.org/10.1130/2020.2544(02))

Appendix 1: Whole-rock lithogeochemistry data of samples from the Long Harbour–Placentia area.

Lab#	Dolerite 10740338 19AM012A	Assemblage 1								Assemblage 2		
		8941345 HS17-093	10740325 19AM005A01	10740334 19AM008A01	8941359 HS17-092A	10740333 19AM007B01	10740335 19AM009A01	10740336 19AM009B01	8941358 HS17-091C	8941355 HS17-094	10740326 19AM006A01	
Mg#	52.75	39.21	42.67	39.6	62.77	9.99	39.51	49.74	47.77	57.09	52.25	
SiO ₂	48.46	65.24	65.28	61.9	42.18	47.94	50.65	53.28	47	48.04	47.32	
Al ₂ O ₃	15.29	15.4	11.89	15.21	17.6	19.43	14.98	15.17	16.1	14.93	16.9	
Fe ₂ O ₃ T	12.4	3.93	3.62	5.62	12.36	8.03	12.31	11.17	12.02	12.18	11.91	
Fe ₂ O ₃	3.86	2.66	0.92	2.7	5.8	7.21	11.22	9.12	2.81	2.73	6.34	
FeO	7.69	1.14	2.43	2.63	5.91	0.74	0.98	1.85	8.29	8.51	5.02	
FeOT	11.16	3.54	3.26	5.06	11.12	7.23	11.08	10.05	10.82	10.96	10.72	
MgO	6.99	1.28	1.36	1.86	10.52	0.45	4.06	5.58	5.55	8.18	6.58	
CaO	5.38	4.6	5.62	1.77	7.16	12.6	8.85	2.99	4.62	7.38	3.95	
Na ₂ O	5.07	1.62	1.97	4.02	1.4	2.68	3.84	1.94	3.23	2.81	4.39	
K ₂ O	0.11	3.65	2.32	3.31	1.18	1.98	0.65	4.85	2.77	0.45	0.82	
TiO ₂	1.424	0.622	0.477	0.853	1.52	0.923	1.115	1.178	1.787	1.787	1.211	
MnO	0.225	0.09	0.202	0.123	0.331	0.121	0.195	0.131	0.276	0.224	0.177	
P ₂ O ₅	0.15	0.093	0.083	0.236	0.391	0.109	0.165	0.226	0.293	0.261	0.225	
Cr	229	6	16	6	126	22	81	77	82	155	96	
Zr	82	213	224	162	133	169	73	91	102	94	72	
Ba	193	1327	706	685	835	301	230	3069	5035	283	462	
Be	0.6	2	1.7	1.5	1.4	1.4	0.7	1	1.7	0.6	0.7	
Sc	33.4	13.8	9.6	21.8	32.5	23.1	45	40.8	41.4	38.3	38.2	
LOI	4.12	1.87	6.63	3.17	5.49	4.28	2.78	3.5	5.2	3.61	4.77	
Total	99.61	98.39	99.46	98.07	100.13	98.53	99.58	100.02	98.85	99.85	98.24	
As	6	4	2	3	13	13	307	21	4	6	3	
Co	48	7	8	11	49	6	37	38	36	46	44	
Cu	162	11	19	10	7	-1	2	16	124	115	106	
Li	37.9	17.7	15.2	20.3	68.6	3.4	17.3	44.9	38	33.7	21.6	
Ni	80	8	9	9	90	28	24	29	32	83	46	
Pb	-1	8	20	-1	2	12	-1	-1	1	-1	-1	
Rb	7	131	68	144	14	72	17	148	57	13	31	
S	77	-5	47	19	-5	9	-5	11	-5	-5	17	
V	282	55	48	137	251	124	106	282	351	302	295	
Zn	94	81	74	85	95	27	64	71	85	93	87	
Ga	17	17	19	21	21	30	13	14	17	15	16	
Ge	3	2	2	1	3	3	2	1	2	2	-1	
Sr	244	372	209	37	295	1406	381	287	161	363	334	
Y	19	27	33	25	31	37	16	20	23	21	18	
Nb	7.5	9.3	10.2	7.2	4.6	7.4	1.6	3.4	4.6	4.8	3.7	
Sn	1	2	3	2	24	3	1	2	1	-1	2	
Cs	1.6	16.1	3	5.9	0.8	3.2	1.1	14.3	1.5	0.8	1.5	
La	5.5	37.5	47.7	19.5	22.3	30.1	10.8	11.8	13.7	11.2	8.8	
Ce	18	80.4	107.6	50.6	40.7	59.6	23.8	31.2	29.1	24.4	22.9	
Pr	2.5	10.2	13.4	6.8	6.1	7.9	3.5	4.2	3.9	3.4	3.1	
Nd	12.1	39.4	54.1	28.9	26.4	34.8	15.8	19.3	18.3	16.2	14.7	
Sm	3.4	8.2	12.2	6.2	6.5	8.2	3.9	4.7	4.8	4.1	3.7	
Eu	1.27	2.08	2.8	1.52	2.03	2.48	1.21	1.53	3	1.4	1.27	
Gd	3.9	6.7	9.6	5.3	6.7	7.9	3.8	4.4	4.9	5	4	
Tb	0.6	1	1.4	0.8	1.1	1.2	0.5	0.7	0.8	0.7	0.6	
Dy	3.9	5.4	7	4.6	6.1	7.1	3.3	4.1	5	4.3	3.7	
Ho	0.7	1.1	1.2	0.9	1.2	1.4	0.6	0.8	0.9	0.9	0.7	
Er	2.1	3.1	3.6	2.9	3.5	4.1	1.9	2.4	2.8	2.5	2.1	
Tm	0.26	0.43	0.51	0.43	0.46	0.57	0.23	0.32	0.34	0.31	0.29	
Yb	1.8	3.1	3.7	3.2	3.1	4	1.7	2.3	2.4	2.3	2	
Lu	0.23	0.49	0.56	0.46	0.46	0.55	0.23	0.32	0.38	0.36	0.28	
Hf	2.1	5.7	6.3	4.8	3.2	5	1.6	2.6	2.5	2.4	2	
Ta	-1	1.4	-1	-1	-1	-1	-1	-1	-1	-1	-1	
W	-1	-1	1	-1	-1	-1	-1	-1	-1	-1	-1	
Tl	-0.1	-0.1	-0.1	-0.1	-0.1	-0.1	-0.1	-0.1	-0.1	-0.1	-0.1	
Bi	0.7	-0.5	0.7	1	-0.5	-0.5	1.6	1.1	-0.5	-0.5	-0.5	
Th	0.8	12.3	11.4	10.7	2.9	7.4	2.3	3.7	1.4	1.1	1.3	
U	0.2	2.8	2.4	2.6	1.1	2	0.4	0.7	0.4	0.3	0.3	
Ag	0.2	-0.1	-0.1	-0.1	-0.1	-0.1	-0.1	0.1	-0.1	-0.1	0.1	
F	217	201	277	291	424	104	275	287	453	219	123	

Appendix 1 Continued: Whole-rock lithogeochemistry data of samples from the Long Harbour–Placentia area.

Lab#	Assemblage 2				Assemblage 3							
	10740327 19AM006A02	10740331 19AM007A01	10740332 19AM007A02	10740328 19AM006B01	10740329 19AM006B02	10740324 19AM001A01	10740337 19AM011A01	10740346 19AM018A01	10740347 19AM018A02	10740348 19AM018A03		
Mg#	49.11	55.25	58.21	63.29	56.34	16.1	57.15	53.46	59.9	50.54		
SiO ₂	45.87	47.55	58.18	43.95	44.84	57.82	43.01	48.64	48.65	48.66		
Al ₂ O ₃	17.22	16.75	14.77	13.82	15.75	14.7	13.6	15.1	16.35	15.54		
Fe ₂ O ₃ T	12.05	12.16	7.78	12.57	11.42	10.32	12.64	9.5	6.63	11.05		
Fe ₂ O ₃	6.08	6.31	2.64	4.06	3.25	8.83	8.82	6.97	4.4	8.51		
FeO	5.38	5.26	4.63	7.66	7.36	1.34	3.44	2.28	2	2.29		
FeOT	10.84	10.94	7	11.31	10.28	9.29	11.37	8.55	5.97	9.94		
MgO	5.87	7.58	5.47	10.94	7.44	1	8.51	5.51	5	5.7		
CaO	5.48	3.3	5.01	7.85	4.89	2.11	9.89	4.93	5.38	3.87		
Na ₂ O	4.95	4.88	4.38	2.42	4.23	4.62	2.68	4.27	4.75	5.46		
K ₂ O	0.96	1.32	2.14	0.64	0.89	2.72	1.19	2.32	3.06	1.47		
TiO ₂	1.241	1.37	0.681	2.063	2.452	2.644	2.977	2.544	2.873	2.688		
MnO	0.201	0.198	0.139	0.189	0.17	0.075	0.23	0.179	0.155	0.162		
P ₂ O ₅	0.235	0.243	0.08	0.416	0.546	0.563	0.757	0.794	0.946	0.885		
Cr	93	130	126	278	188	31	405	67	2	3		
Zr	75	75	89	134	167	215	202	244	301	284		
Ba	803	1004	719	658	523	2222	728	622	711	382		
Be	0.9	0.7	0.7	1.2	1	1.6	1.7	1.8	2.1	1.9		
Sc	39.2	36.6	28.1	26.1	27.4	15.3	28.1	20.6	13.9	13.4		
LOI	5.17	4.22	2.34	4.73	7.24	1.98	4.28	4.31	4.24	3.46		
Total	99.24	99.57	100.97	99.59	99.88	98.55	99.76	98.09	98.02	98.95		
As	5	6	3	9	8	7	13	12	7	5		
Co	45	52	34	64	47	16	51	35	31	28		
Cu	61	23	71	58	97	32	12	27	75	137		
Li	18	29.9	15.4	25.3	30.8	17.5	39.2	29.5	25.6	32.8		
Ni	46	75	68	199	97	16	129	53	25	15		
Pb	-1	-1	3	-1	41	-1	-1	-1	-1	-1		
Rb	31	49	46	13	26	83	21	52	65	34		
S	15	9	23	25	69	406	28	14	23	33		
V	298	292	173	227	237	205	244	249	252	361		
Zn	95	86	60	89	145	58	81	70	62	67		
Ga	18	15	15	18	19	18	20	21	19	19		
Ge	1	-1	2	1	1	2	3	2	2	3		
Sr	301	348	274	308	247	165	652	402	423	319		
Y	19	19	24	18	20	34	22	28	33	27		
Nb	3.6	3.4	3.9	24.8	35	45.3	44	37.1	62.3	53		
Sn	2	1	2	2	2	3	2	4	3	4		
Cs	1.2	2.5	0.9	1.5	3.3	4.6	0.8	2.6	2.8	1.8		
La	10.2	6	13.7	19.9	24	61.3	38.8	38.6	40.8	42.6		
Ce	23.9	19.7	32.9	45.1	52.9	126.1	86.1	82.6	93.4	95.7		
Pr	3.3	2.8	4	5.6	6.5	14.5	10.8	10	12	11.8		
Nd	15.8	13.8	16.5	24.5	27.7	59.4	44.9	42.4	51.4	49.2		
Sm	3.8	3.7	3.9	5.5	5.9	10.8	8.8	8.6	10.3	9.4		
Eu	1.37	1.33	1.05	1.91	1.79	2.81	2.62	2.93	2.72	2.47		
Gd	4.1	4	4.3	5	5.6	9.2	7.2	7.6	8.7	7.9		
Tb	0.6	0.6	0.7	0.7	0.8	1.3	1	1.1	1.2	1.1		
Dy	3.9	3.9	4.6	4.1	4.6	6.9	5.1	6	6.8	6		
Ho	0.8	0.7	0.9	0.7	0.8	1.2	0.9	1.1	1.1	1.1		
Er	2.3	2.2	2.8	2	2.3	3.3	2.3	3.1	3	2.9		
Tm	0.3	0.29	0.41	0.25	0.28	0.39	0.29	0.42	0.38	0.39		
Yb	2.1	2	2.9	1.6	1.9	2.6	1.9	2.7	2.8	2.5		
Lu	0.3	0.26	0.42	0.21	0.24	0.36	0.24	0.38	0.36	0.35		
Hf	2	1.8	2.8	3.4	4.1	5.3	5.2	5.8	6.8	6.4		
Ta	-1	-1	-1	1.2	1.9	2.8	2.5	2.7	3.9	3.5		
W	6	-1	8	-1	3	-1	4	6	1	-1		
Tl	-0.1	-0.1	-0.1	-0.1	-0.1	-0.1	-0.1	-0.1	-0.1	-0.1		
Bi	-0.5	1.2	0.6	-0.5	1.2	0.8	1.5	0.5	-0.5	2.4		
Th	1.4	0.9	7	2.4	3	3.3	3.8	3.9	3.8	3.8		
U	0.4	0.3	1.8	0.7	0.9	1.6	1.4	2.9	1.2	0.7		
Ag	-0.1	0.2	0.2	-0.1	-0.1	-0.1	-0.1	-0.1	-0.1	-0.1		
F	147	152	166	268	271	495	569	515	544	527		